Title
Topics in Non-Equilibrium Dynamics and the Emergence of Spacetime

Author
Engelhardt, Dalit

Publication Date
2016

Peer reviewed|Thesis/dissertation

University of California
Los Angeles

Topics in Non-Equilibrium Dynamics and the Emergence of Spacetime

A dissertation submitted in partial satisfaction
of the requirements for the degree
Doctor of Philosophy in Physics

by

Dalit Engelhardt

2016

Abstract of the Dissertation

Topics in Non-Equilibrium Dynamics and the Emergence of Spacetime

by

Dalit Engelhardt

Doctor of Philosophy in Physics

University of California, Los Angeles, 2016

Professor Per J. Kraus, Chair

The Anti-de Sitter / Conformal Field Theory (AdS/CFT) correspondence that arises in string theory has had implications for the study of phenomena across a range of subfields in physics, from spacetime geometry to the behavior of condensed matter systems. Two major themes that have featured prominently in these investigations have been the behavior of systems out of equilibrium, and the emergence of spacetime. In this thesis, aspects of these themes are considered and analyzed.

The question of equilibration and thermalization in 2D conformal field theories is addressed and refined via a number of observations about local versus global thermalization in such systems, the validity of particular diagnostics of thermalization, the dependence of the equilibration behavior of a conformal field theory on its operator spectrum, and the holographic dual of the generalized Gibbs ensemble that is of interest in studies of equilibration in systems with a large number of conserved quantities. A formalism for analyzing the non-equilibrium dynamics of 1+1-dimensional conformal field theories is discussed, and its physical relevance is motivated with an example connecting such a system to an experimental system that exhibited unusual equilibration behavior. Qualitative agreement is demonstrated between the CFT picture and the experimental observations.

The emergence of spacetime geometry from quantum entanglement, while largely a

byproduct of considerations from holographic dualities, has also been proposed to have a direct, non-holographic manifestation. Here a particular realization of such a direct emergence is presented through a demonstration that, in the presence of quantum entanglement alone, certain observations of electric fields in the entangled system appear qualitatively the same as the corresponding observations in a physically-connected geometric spacetime, so that the entanglement effectively mimics particular features associated with geometric connectivity.

The dissertation of Dalit Engelhardt is approved.

Terence Chi-Shen Tao

Michael Gutperle

Eric D'Hoker

Per J. Kraus, Committee Chair

University of California, Los Angeles

2016

To my family

Table of Contents

List of Figures

Acknowledgments

I am grateful to my advisor, Per Kraus, for his support over the years and for the useful and instructive discussions throughout my PhD that have helped sharpen my understanding of high energy theory. I am also grateful to my collaborators – Jan de Boer, Ben Freivogel, and Nabil Iqbal – for the interesting work that we have done together, for their contributions to my knowledge, and for helping me grow as a researcher.

I would also like thank Eric D'Hoker, Michael Gutperle, and Terence Tao for serving on my committee.

I want to extend a very special thanks to my sister, Netta Engelhardt, who is the best combination of loving sister, fellow researcher, and supportive friend that I could have.

My knowledge of physics would not be what it is today without the many interesting and instrumental conversations and discussions that I have had with many people along the way. I would particularly like to thank Rob Myers for his guidance and our many discussions during my time at Perimeter Institute. I would also like to thank for many interesting and insightful discussions Pablo Bueno, Damian Galante, Matthew Lippert, Marco Meineri, Gabor Sarosi, Wilke van der Schee, Antony Speranza, and others who were my contemporaries during my visits at Perimeter Institute and the University of Amsterdam, as well as the graduate student community at UCLA.

Finally, I could not have done any of this without the loving support of my family: my sister, Netta, as I have noted above; my grandparents, whose faith in me has been instrumental in this journey; and my parents, whose encouragement and support have been essential during this endeavor, and who have always inspired me to pursue my deepest interests and to follow my own path.

The work in this dissertation has been supported by the NSF Graduate Research Fellowship and Graduate Research Opportunities Worldwide (DGE-0707424), NSF grant PHY-

1313986, the Netherlands Organisation for Scientific Research (NWO), and the University of Amsterdam.

Vita

2014 MS, Physics, University of California, Los Angeles, CA.

2009 MS, Pure Mathematics, Imperial College, London, UK.

2008 BA, Physics and Mathematics, Boston University, MA.

Publications

J. de Boer and D. Engelhardt, "Comments on Thermalization in 2D CFT", arXiv:1604.05327 (*preprint*).

D. Engelhardt, "Quench dynamics in confined 1+1-dimensional systems", *J. Phys. A* **49** (2016) 12LT01 [arXiv:1502.02678].

D. Engelhardt, B. Freivogel, and N. Iqbal, "Electric fields and quantum wormholes", *Phys. Rev. D* **92** (2015), no. 6 064050, [arXiv:1504.06336].

H.-C. Cheng, D. Engelhardt, J. F. Gunion, Z. Han, and B. McElrath, "Accurate Mass Determinations in Decay Chains with Missing Energy", *Phys. Rev. Lett.* **100** (2008) 252001, [arXiv:0802.4290].

CHAPTER 1

Introduction

The nearly two decades that have passed since the discovery of the Anti-de Sitter / Conformal Field Theory (AdS/CFT) correspondence [1] have brought about a veritable revolution in our perception of concepts at the heart of both quantum and gravitational phenomena. While a theory of quantum gravity remains elusive, developments ensuing from the implications of the AdS/CFT correspondence have fundamentally altered our understanding of the nature of spacetime, locality, causality, the role of quantum information in a unified theory of quantum gravity – and the connections between these concepts and others. They have further contributed to an improved ability to describe systems that defy the tools of perturbation theory due to their strong coupling, leading to a flourishing research effort into condensed matter systems through the use of tools from general relativity.

In this thesis, two major themes that have emerged from research into holograpic dualities are considered. The first of these – the behavior of systems out of equilibrium – is a subject that extends far beyond holography and is of interest for practically any physical system, as our world by and large is not in equilibrium. As pervasive as non-equilibrium behavior is, however, there are surprisingly few tools at our disposal for analyzing and modeling such systems. Holography has given us new perspectives on and tools for investigating non-equilibrium behavior and has given rise to a large research effort employing gravitational setups for studying non-equilibrium quantum field theories. The focus of this thesis is on the non-equilibrium behavior of certain systems in one spatial dimension, and to that purpose both holographic and non-holographic considerations will be employed. One-dimensional systems have been shown both theoretically and experimentally to exhibit rather diverse

behavior out of equilibrium, and research into these systems continually reveals new and interesting physics.

The second theme is at the core of efforts designed to understand the fundamental nature of a unified quantum theory of gravity. The implication of the holographic duality that – at least in principle – all information about a gravitational theory in a higher-dimensional spacetime is contained within a lower-dimensional quantum field theory has led to the idea that spacetime geometry and hence gravitational dynamics *emerge* from the quantum theory in a similar spirit to the emergence of complex dynamics from elementary interactions. In particular, there has been accumulating tantalizing evidence that quantum information may hold the key to understanding this emergence, as particular properties and objects of quantum information in field theory have been shown to be dual to constructs in the corresponding gravitational theory [2–4]. Many recent efforts have centered on "reconstructing" the gravitational theory in the bulk and hence the bulk geometry by studying quantum entanglement and other information theoretic objects in the dual quantum field theory[1]. Interestingly, there may also be a very direct, non-holographic way in which spacetime emerges from quantum behavior. This type of non-holographic emergence was first suggested in the work of Maldacena and Susskind [12]; in this thesis a specific manifestation of this type of emergence is shown. This direct type of emergence may provide profound clues for the connections between spacetime geometry, quantum theory, and a unified framework encompassing the two.

1.1 The AdS/CFT duality and spacetime emergence

Recent work in string theory has advanced our understanding of the connection between quantum theory and gravity through the idea of holography. The holographic principle is the idea that in a quantum theory of gravity, all information about a particular region is encoded in the boundary of that region. This idea has its origins in black hole thermodynamics and

[1]There is a vast literature dedicated to this subject; for some earlier references see, e.g., [5–11].

the realization that the entropy of a black hole scales as its horizon area A [13, 14]

$$S_{\rm BH} = \frac{c^3 A}{4G\hbar},$$

rather than its volume, as would be expected from statistical mechanics[2]. In other words, the scaling of the entropy in the d-dimensional gravitational theory is that which would be expected for a $d-1$-dimensional local quantum field theory instead. The interpretation that phenomena in the higher-dimensional theory should have a complete description in terms of the degrees of freedom of a lower-dimensional theory, the so-called holographic principle for its analogy with the workings of a hologram, was elucidated by 't Hooft [15] and Susskind [16] (see also [17]) and has had a profound effect on subsequent work in quantum gravity.

Still two decades earlier than these developments, it was suggested by 't Hooft [18] that large-N gauge theory, where N is the rank of the gauge group, is equivalent to a string theory. The idea behind this equivalence is that any diagram in the gauge theory can be expanded as

$$\sum_{g=0}^{\infty} N^{2-2g} f_g(\lambda) \tag{1.1.1}$$

where the 't Hooft coupling λ is defined as $\lambda \equiv g_{YM}^2 N$, where g_{YM} is the coupling constant (the subscript YM denoting Yang-Mills), g is the genus of the surface corresponding to the diagram, and f_g is some polynomial in λ. By identifying the string coupling constant g_s with $1/N$ the form of the expansion (1.1.1) is seen to be the same as that of the perturbative expansion in string theory with closed oriented strings. Note that at large N the expansion (1.1.1) will be dominated by surfaces of small g, i.e. by planar diagrams, proportional to N^2. This large N limit would correspond to small g_s, i.e. a weakly-coupled string theory.

The holographic principle and 't Hooft's equivalence of gauge and string theory found specific manifestation in Maldacena's groundbreaking proposal in 1997, arrived at by examining a particular limit of string theory, of a duality in the large-N limit between type IIB supergravity compactified on a direct product of five-dimensional Anti-de Sitter space with a

[2] $\sqrt{G\hbar/c^3}$ is the Planck length.

sphere, $\mathrm{AdS}_5 \times S^5$ and $\mathcal{N} = 4$ supersymmetric Yang-Mills (SYM) $SU(N)$ gauge theory in four dimensions. Anti-de Sitter (AdS) space is a maximally-symmetric spacetime with negative cosmological constant, and $\mathcal{N} = 4$ SYM $SU(N)$ gauge theory is a quantum field theory that is invariant under a type of transformations known as conformal (angle-preserving) transformations. This dual field theory lives on a spacetime conformal to that of the AdS boundary and hence can be regarded as "living on the boundary" of the AdS spacetime. Constructs in the "bulk" of AdS are thus dual to constructs in the boundary theory. The string coupling g_s, string length l_s, and the curvature radius L of AdS are identified in this correspondence with the gauge theory parameters g_{YM} and N as $g_s = g_{YM}^2$ and $(L/l_s)^4 = 4\pi g_{YM}^2 N = 4\pi\lambda$.

The AdS/CFT is a strong/weak duality: SYM theory can be treated perturbatively if $g_{YM}^2 N \ll 1$ and hence $\lambda \ll 1$, but this is also the regime at which stringy effects become very strong in the bulk, since $L \ll l_s$; conversely, taking $\lambda \gg 1$ reduces to a classical gravity theory in the bulk and a strongly-coupled gauge theory on the boundary. In its weakest form, the duality holds in the limit of $N \to \infty$ and $\lambda \to \infty$, so that the equivalence is between type IIB supergravity and the gauge theory at strong coupling. A somewhat less strong form is obtained by taking $N \to \infty$ but keeping λ finite. In its strongest form, this exact equivalence is conjectured to hold for any N and g_s and hence for a fully quantum string theory on the (asymptotically) AdS bulk spacetime. While the duality has successfully undergone various checks to date, its strong form is difficult to prove due to the present lack of a description of non-perturbative string theory.

Since Maldacena's proposal of the AdS/CFT correspondence this duality has expanded to include a larger class of spacetimes and boundary field theories in other dimensions that are conjectured to be dual to each other, leading to the more general term of "gauge/gravity duality." The power of these dualities is in their potential to use gravitational objects in a higher-dimensional theory with dynamical gravity to compute quantities in a lower-dimensional quantum field theory that cannot normally be computed by methods available to quantum field theory; conversely, the duality has the potential to uncover ill-understood phenomena in string theory via gauge theory calculations.

In principle, since all information in the bulk spacetime in which the gravitational theory lives is believed to be encoded in the dual field theory, it should be possible to reconstruct the gravitational theory of the bulk from known quantities in the dual field theory, and vice versa. Work subsequent to the original AdS/CFT proposal established a dictionary relating fields in the bulk gravitational theory to operators in the boundary field theory [19, 20]. The statement of the duality was cast as an equivalence between the partition functions of the bulk gravitational theory and the boundary quantum field theory: for a massless scalar field ϕ in AdS_{d+1} whose restriction to the boundary of AdS is ϕ_0 we have that

$$Z(\phi_0) = \left\langle \exp \int_{\mathbf{S}^d} \phi_0 \mathcal{O} \right\rangle_{\text{CFT}}, \tag{1.1.2}$$

where $Z(\phi)$ is the partition function of the gravitational theory in AdS and on the right-hand side we have the generating functional for correlation functions in the CFT on the boundary $\mathcal{S}^d$, where $\mathcal{O}$ is a field in the CFT. In this expression, the boundary field ϕ_0 acts as a source for the operator $\mathcal{O}$, and bulk fields are thus in one-to-one correspondence with boundary field theory operators. In principle, the equivalence (1.1.2) can be used to compute various correlation functions, permitting a direct translation between the observables of a given theory and its holographic dual [19, 20]. The equivalence of this relation, referred to as the GKPW dictionary, to the "extrapolate" version of the AdS/CFT dictionary [21] was conjectured in [21] and shown in [22, 23]. The extrapolate dictionary gives the correlation functions of operators in the CFT in terms of the asymptotic behavior of bulk field correlators:

$$\langle \mathcal{O}(x_1)...\mathcal{O}(x_n)\rangle_{CFT} = \lim_{z\to 0} z^{-n\Delta} \langle \phi(x_1, z)...\phi(x_n, z)\rangle_{bulk}$$

where x_i are boundary coordinates and the bulk coordinate $z \to 0$ at the AdS boundary. Δ is the conformal dimension of the CFT operator and is related to the mass of the scalar field ϕ as

$$\Delta = \frac{d}{2} + \sqrt{\frac{d^2}{4} + m^2}.$$

Note, however, that both of these dictionaries involve the asymptotic behavior of bulk fields, and, in fact, a direct relation between bulk fields and boundary operators is only well-understood near the boundary of the bulk spacetime, i.e. only in the regime in which the location of the bulk field approaches the boundary where the field theory lives. In other words, the dictionary is "sharp" near the boundary of the spacetime, but, in general cases[3], further into the bulk it becomes less clear how fields can be related to boundary operators. This difficulty arises because the boundary is not a Cauchy surface for the bulk, and evolving the boundary fields into the bulk is therefore a nonstandard Cauchy problem [25, 26]. While obtaining a dictionary that extends this relation into the bulk would be an ideal goal, it remains elusive in all but the simplest spacetimes. As a result, much of the effort on relating the bulk gravitational theory to the dual field theory has focused on the use of probe objects that have a dual interpretation in both theories. Examples of such probe objects include types of geodesics that are related to field theory correlators and extremal surfaces that are related to entanglement entropy [2–4] in the boundary field theory. This latter work, in particular, has been critical in driving forward the idea that spacetime geometry emerges from quantum entanglement.

Quantum entanglement is the presence of non-trivial correlations between different systems that are spatially arbitrarily far apart. It is a quantum mechanical phenomenon that has no classical counterpart and is an active area of research in multiple disciplines, including theoretical high energy physics, quantum information theory, and quantum cryptography. The idea that the entanglement of quantum fields is connected to a physical emergent spacetime geometry arose both in the context of holographic dualities as well as non-holographically. The general idea of emergence of a higher-dimensional theory from a lower-dimensional theory naturally follows from the holographic principle, but the specific role of entanglement in this emergence was not immediately apparent in the early years of the AdS/CFT correspondence. This connection was illuminated by Van Raamsdonk in [5, 6] and was followed in subsequent years by a flurry of literature aimed at developing a better understanding of

[3] In pure global AdS a map between bulk and boundary fields has been found explicity [24].

this connection, including efforts at perturbative derivations of the Einstein equations of the bulk gravitational theory from relations satisfied by the entanglement in the dual quantum field theory [11, 27, 28]. While research efforts have shown to date that there are remarkable connections between entanglement and spacetime geometry, an understanding of the underlying mechanism of emergence so far remains elusive.

A recent proposal by Maldacena and Susskind [12], made in the context of the black hole information paradox debate, suggested that any entangled matter is connected by some type of wormhole, which is classically an Einstein-Rosen bridge but that in general may be a highly quantum object. This type of emergence is non-holographic; in this thesis such non-holographic emergence is considered and a direct sense is shown in which a setup consisting of purely entanglement rather than any geometric connection reflects certain features that are normally expected only in a connected spacetime. More precisely, there is a particular sense in which a theoretical observation of an electric field penetrating a geometrical wormhole and that of an electric field threaded through a disconnected configuration of two entangled systems that are arbitrarily far apart appear very similar. This presents an intriguing finding regarding the behavior of entangled matter and the notion of the emergence of spacetime geometry from quantum mechanical behavior.

1.2 Non-equilibrium dynamics

Holographic dualities have given us a window into the physics of systems perturbed away from equilibrium, whose modeling is a challenging problem in all but a limited number of cases. The time evolution of systems out of equilibrium has been shown to exhibit a rich array of behaviors that depend on the type of initial perturbation and the characteristics of the systems. At asymptotically late times, however, they are generically expected to exhibit behavior characteristic of thermal equilibrium, regardless of the short-time behavior following the perturbation, so long as the perturbation injects sufficient energy into the system. This process of "thermalization" is central to research in both high energy physics

and statistical mechanics. One of the successes of holography has been the recasting of the investigation of this process as the study of dual gravitational phenomena. In particular, a finite temperature in the boundary field theory is understood to be dual to a black hole in the asymptotically-AdS bulk spacetime, though this statement should be qualified by noting that the gravitational solution may be thermal AdS rather than a black hole. The equivalence between a thermal state in the CFT and black holes in the bulk can be seen by observing that taking the time direction of the boundary manifold to be a circle of size β, the inverse temperature, puts the CFT at finite temperature. This boundary manifold structure imposes a boundary condition on the bulk metric, and in the classical gravity limit the bulk solutions to Einstein's equations satisfying this boundary condition can be found. In AdS_5 these may be large black holes, small black holes, or thermal AdS (i.e. AdS filled with thermal radiation). It can be shown that the large black hole solutions have a lower free energy and therefore dominate over small black holes at any temperature; on the other hand, whether the large black hole or thermal AdS is dominant depends on the temperature. At a certain critical temperature there is a first order phase transition, the Hawking-Page phase transition [29], between the low-temperature thermal AdS phase and the higher-temperature black hole phase. On the dual CFT side, this transition has been interpreted as a confinement/deconfinement phase transition [30]. This picture qualitatively also carries over to other dimensions. In AdS_3/CFT_2, which will be of special interest to the discussion of Chapter 2, the transition is between thermal AdS_3 and the BTZ black hole [31, 32].

The process of thermalization in the field theory is thus dual to the formation of a black hole in the bulk, and sudden changes in the system's Hamiltonian parameters – known as quantum quenches – result in the injection of energy into the bulk. Since the boundary conditions of AdS spacetime are such that AdS is essentially a "closed box," this energy cannot dissipate at the asymptotic boundaries and is instead reflected at the boundaries. The general expectation is thus that when energy is injected into the bulk sufficiently large gravitational backreaction will eventually be built up to induce black hole collapse [33, 34].

While research into the possibility that stable, oscillating matter configurations in AdS that do not collapse to a black hole may exist is ongoing (this is discussed further in Chapter. 2), analytical solutions above the BTZ mass threshold that do not rely on highly simplifying assumptions and that exhibit undamped oscillations at asymptotically late times have not yet been found. Rather, as noted above, the generic expectation from AdS physics is that systems dual to classical gravitational asymptotically-AdS spacetimes should thermalize. On the other hand, the past decade has seen accummulating experimental and theoretical evidence that the expectation that all systems equilibrate to a simple thermal state may be misleading in 1+1-dimensional systems, where in some cases thermalization appears to be inhibited entirely, and the systems instead appear to retain memory of their initial state[4]. Such an absence of thermalization has been attributed to the presence of a large number of conserved charges in those systems and the associated notion of "quantum integrability," and much work has been devoted in recent years toward understanding the out-of-equilibrium behavior of such systems.

A classical system with n degrees of freedom is (Liouville) integrable if it has n independent first integrals of motion that all Poisson-commute with each other. This implies that the differential equations describing the system can be solved analytically; their solutions form phase-space trajectories on invariant tori and remain quasi-periodic for all time. Such systems are therefore non-ergodic as they fail to explore their full phase space even at asymptotically late times; this is in contrast to the usual case, where the nonlinear differential equations cannot be solved analytically and generally exhibit chaotic behavior. Translating the notion of classical integrability to the quantum case is far from straightforward and there is no standard definition of what it means for a system to be quantum integrable [39, 40]. Among properties that have generally been associated with quantum integrability in the literature are that the system possesses a maximal set of independent commuting operators (in direct analogy to the classical case)[5], it is exactly solveable (e.g. via the Bethe ansatz [41]),

[4] See [35–38] for reviews.

[5] However, it was argued in [39, 40] that this definition effectively leads any quantum system to be characterized as integrable and that it is therefore inadequate.

or that it exhibits non-diffractive scattering.

The large number of local conserved quantities that these systems possess is believed to prevent their thermalization to the canonical (Gibbs) ensemble. However, it has been proposed [42] that relaxation to a maximal entropy state still occurs, and that the resulting ensemble is instead a generalized Gibbs ensemble with density matrix

$$\hat{\rho} = \frac{1}{Z} \exp\left[-\sum_m \lambda_m \hat{\mathcal{I}}_m \right] \tag{1.2.1}$$

where $\left\{ \hat{\mathcal{I}}_m \right\}$ is the full set of integrals of motion, $Z = \mathrm{Tr}\left[\exp\left[-\sum_m \lambda_m \hat{\mathcal{I}}_m \right] \right]$ is the partition function, and λ_m are Lagrange multipliers that are fixed by the requirement that expectation values of conserved quantities remain constant at their initial values. When there are very few conserved quantities this ensemble reduces to the usual canonical (if the only conserved quantity is energy) or grand-canonical ensemble (if both energy and particle numbers are conserved).

Much of the research regarding integrability and experimental observations of non-thermalization have been in 1+1-dimensional systems. The behavior of many 1+1-dimensional systems at criticality is described by CFTs, leading to the natural question of whether such non-thermalization is observed for those CFTs, and, if so, whether there is a potential conflict with the expectation from holography of generic thermalization in the CFT. This is addressed in this thesis via a combination of techniques from CFT and from holography. Notably, CFTs with classical holographic duals are expected to have very large central charge c, whereas integrable systems have traditionally been discussed in the context of specific perturbations of conformal minimal models, for which $c < 1$. These differences, and their implications for thermalization, are discussed in this thesis, along with several other aspects of thermalization in 2D CFT that are crucial for an understanding of non-equilibrium behavior in these theories.

1.3 Outline of thesis

These issues are considered in Chapters 2 and 3. In Chapter 2 several aspects of thermalization in 2D CFT are addressed via tools from both holography and the CFT boundary state formalism (which is reviewed in that chapter). The distinction between global and local thermalization is considered and sharpened, and the CFT stress tensor is shown to be an insufficient diagnostic of global thermalization. The question of revivals and thermalization in CFTs of different central charges is then addressed by examining the time dependence of correlation functions in various states in rational and non-rational CFTs. Since all 2D CFTs have an infinite set of commuting conserved charges, generic initial states might be expected to give rise to a generalized Gibbs ensemble as described above (1.2.1). The holographic dual of the GGE is constructed and shown, to leading order, to still be described by a BTZ black hole.

In Chapter 3 the physical relevance of the CFT boundary state quench setup is addressed through a compelling physical example of the applicability of boundary states to realistic systems. A model is presented of the conformally-invariant analog of the "Quantum Newton's Cradle" experiment [43]. This near-integrable system was observed not to thermalize on experimental time scales, and the results from the CFT model are shown to qualitatively agree with the experimental observations in revival times and distributions. Beyond ascribing physical significance to the boundary state model, the demonstrated success of this approach is suggestive of special features of integrable systems with respect to their conformally-invariant counterparts.

Chapter 4 is concerned with the question of spacetime emergence in a direct, rather than holographic, sense as discussed above. It is demonstrated within low-energy effective field theory how entanglement alone can in fact mimick a particular feature that is unique to a wormhole geometry. The sense in which the geometry emerges is in the manner in which the entanglement between charged scalar fields in disconnected configurations gives rise to behavior that is shown to be indicative of geometric connectivity. In particular, the ability

to pass an electric field through a wormhole is such an indication; this notion is quantified by defining a "wormhole susceptibility" that measures the ease of passing through an electric field, and this quantity is shown to exhibit qualitatively the same behavior in the purely entangled (and geometrically disconnected) configuration as in the gravitational geometric (Einstein-Rosen bridge) case. In other words: electric fields can thread quantum wormholes.

1.4 Attributes and permissions

Chapter 2 is the result of a collaboration with Jan de Boer and is a modified version of [44].

Chapter 3 is a modified version of a publication that has previously appeared in Journal of Physics A [45]. This is an author-created, un-copyedited version of an article published in Journal of Physics A: Mathematical and Theoretical. IOP Publishing Ltd is not responsible for any errors or omissions in this version of the manuscript or any version derived from it. The Version of Record is available online at http://iopscience.iop.org/article/10.1088/1751-8113/49/12/12LT01

Chapter 4 is the result of a collaboration with Ben Freivogel and Nabil Iqbal and is a modified version of a publication that has previously appeared in [46]. It is reproduced here with the permission of the American Physical Society: http://journals.aps.org/copyrightFAQ.html#thesis

CHAPTER 2

Comments on Thermalization in 2D CFT

2.1 Introduction

In this chapter, we consider several aspects of thermalization in 2D CFTs. Thermalization can be investigated from the point of view of a subsystem, where the system is defined to have thermalized if its reduced density matrix is equal to that of a thermal (mixed) state; however, isolated quantum systems starting from a pure quantum mechanical state can also be described as "thermalized" if the expectation values of observables at late times are in agreement with those of a thermal ensemble [47–50].

As discussed in Chapter 1, systems in 1+1 dimensions exhibit varied equilibration behaviors, and whereas generically we expect systems to asymptote at late times to a description in terms of a thermal ensemble, it is clear that certain classes of systems in 1+1 dimensions defy this expectation. The fact that the critical behavior of many 1+1-dimensional systems is described by conformal field theories (CFTs) suggests that there may be qualitative differences between the thermalization behavior of 2D CFTs with their infinite dimensional conformal symmetry as compared to that of higher-dimensional CFTs, where the stress tensor and its descendants are the only conserved currents to be found.

Nonetheless, even for unitary 2D CFTs there are important differences between the behavior of CFTs whose central charge is below or above some critical value c_{crit}, where c_{crit} depends on the chiral algebra of the 2D CFT and determines whether the CFT is rational ($c < c_{\text{crit}}$) or not[1] ($c > c_{\text{crit}}$). For CFTs whose symmetry is only the Virasoro algebra, i.e.

[1] While this appears to be the case in known examples, we are not aware of a rigorous proof of this statement.

with no additional extended symmetries, $c_{\text{crit}} = 1$. In the rational case, the spectrum of the theory consists of a finite number of primaries for the chiral algebra with rational conformal dimensions of the form $\frac{p}{q}$, with integer p, q. For a CFT on a circle of radius R, time translations are thus generated by $U(t) = \exp\left(-it\left(L_0 + \bar{L}_0 - \frac{c}{12}\right)/R\right)$, so that all correlation functions will be periodic in time[2], where the existence of such revivals follows from the rationality of the conformal dimensions in the CFT, and their period depends on the operator spectrum and on the size R of the system. Clearly, theories with $c < c_{\text{crit}}$ do not thermalize, although it is still in principle possible for subsystems to behave approximately as thermal systems for times t that are much smaller than the revival time of the system.

For $c > c_{\text{crit}}$, this argument no longer applies, and there is no *a priori* mechanism to prevent thermalization for generic perturbations. There are nonetheless special states that fail to thermalize in any CFT, the simplest examples being states that are built from descendants of the ground state only. These states are linear superpositions of states with integer conformal dimension, and their period is proportional to the system size L alone. Even in such states, sufficiently small subsystems will exhibit approximately thermal behavior for times $t \ll L$, however globally the system undergoes periodic revivals.

Special descendants of the ground states, coherent states, have a geometric interpretation as conformal transformations of the CFT on the plane or a subspace thereof. In the case of a bounded subspace, such boundary states in the form of a strip or a rectangle have been used to analyze certain quantum quenches and CFT non-equilibrium behavior (see, e.g., [51–58] and the work presented in Chapter 3 of this thesis). In such setups conditions on the Euclidean boundary define the initial conditions of the system, whose time-evolved correlation functions are computed by analytic continuation from Euclidean time. Such states can be understood to define an initial state via a Euclidean path integral over a portion of the boundary, with correlation functions computed by joining together domains representing an in- and an out-state. For example, a path integral over a rectangle with

[2]It should be emphasized that these revivals are different from Poincaré recurrences and occur on far shorter time scales.

suitable boundary conditions on three sides provides a state in the CFT on the interval formed by the remaining side; a correlation function in this state can be computed by joining together such an in-state with an out-state, resulting in a full rectangle[3]. Similarly, in the case of the strip opposite halves represent the in- and out-states. While strip states have been shown to exhibit behavior consistent with thermalization, one has to be careful with CFTs defined on the entire real line. Paraphrasing the result of [56], a conformal compactification of the real line maps it to a finite interval[4], and it maps all of Minkowski spacetime to a causal diamond based on the finite interval. Therefore, measurements in Minkowski space are insensitive to the presence of the boundaries of the interval, which introduce a finite size in the system that determines the period of revivals. The restriction of strip observations to a causal subset thus prevents non-thermal features of such states from being detected. This paper therefore made it clear that the apparent thermalization in strip states observed in [51–54] is due to the restriction to a limited amount of time.

These observations can be further motivated by noting that many features of global thermalization of a CFT, such as the appearance of a suitable coarse-grained entropy, should be conformally invariant. In fact, one could argue that a better (and conformally invariant) definition of thermalization would be to require that expectation values at late times approach those of a thermal state or those of a conformally transformed thermal state. In particular, in holographic theories, where conformal mappings are dual to bulk diffeomorphisms, thermalization invariance under conformal mappings is equivalent to the evident statement that black hole formation (or lack thereof) is diffeomorphism invariant. Since black hole formation following an injection of energy is rather generic in AdS, this calls into question which CFT states do in fact thermalize. As we show here, in non-rational CFTs, i.e. where $c > c_{\text{crit}}$, no revivals would be observed in expectation values of primary operators in general states constructed as linear superpositions of states obtained by local operator insertions.

[3]This is discussed in more detail in Sec. 2.3.

[4]The precise map is $e^{i\tilde{z}} = (e^z - 1)/(e^z + 1)$, where $z \in [-\infty, \infty] \times [0, \pi]$ is the coordinate on the Euclidean strip of infinite spatial extent, and $\tilde{z} \in [0, \pi] \times [-\infty, \infty]$ a coordinate on a finite strip with infinite extent in Euclidean time.

To the extent that the absence of revivals in the system is indicative of its thermalization, this is in line with the expectation from holography.

An interesting additional feature of 2D CFTs is the existence of an infinite number of commuting conserved charges, even when the chiral algebra is just the Virasoro algebra. The lowest two charges are L_0, the zero mode of T, and the zero mode K_0 of $:TT:$. These charges are a quantum version of the infinite number of conserved charges that appear in the KdV hierarchy [59]. One would more generally expect that generic states in a 2D CFT at late times should be describable in terms of a generalized Gibbs ensemble with chemical potentials for all conserved charges instead of the thermal ensemble (see Sec. 1.2). This has indeed been confirmed in [60–62].

A nice heuristic picture of some of the features of thermalization in 2D CFTs arises by assuming that all excitations can be described in terms of free quasi-particles [51, 52, 63, 64]. If after a quench correlated pairs of quasi-particles are locally emitted, the entanglement between an interval of length L and its complement will increase until time $T \sim L/2$ and then remain constant. This picture of growth and saturation is qualitatively in keeping with the holographic predictions [65–68]. In the case of a union of disjoint intervals, on the other hand, the post-quench behavior of the entanglement entropy given by the quasi-particle picture only correctly corresponds to the behavior for $c < c_{\text{crit}}$ [57] systems. There therefore appear to be close connections between integrability, rational conformal dimensions, and the validity of the quasi-particle picture for $c < c_{\text{crit}}$ on the one hand, and between irrational conformal dimensions, lack of integrability, and the breakdown of the quasi-particle picture for $c > c_{\text{crit}}$.

The inhibition of thermalization that we find in rational CFTs by contrast to general CFTs thus further asserts such connections. In this chapter, we clarify some additional aspects of these connections and make contact with the dual holographic picture that they provide. We begin by discussing the holographic dual picture of local thermalization in a pure state and analyze the capacity of the CFT stress tensor for serving as a thermalization diagnostic (Sec. 2.2). We then exploit the conformal invariance of global thermalization

in a CFT by evaluating whether local perturbations of the rectangle state are followed by initial-value revivals of observables at asymptotically-late times; such revivals are indicative of the system's inability to establish an asymptotic thermal state, and we show that as is expected from holography, they naively do not take place for a general (non-rational) CFT (Sec. 2.4). This discussion is preceded by a review of the boundary-state setup and the strip and rectangle states (Sec. 2.3). Finally, we consider the holographic dual of the generalized Gibbs ensemble with chemical potentials for all conserved charges and show that it is still described by the BTZ black hole (Sec. 2.5). We conclude with a discussion of future directions.

2.2 Probes of local and global thermalization

The general thermalization setup is to consider a CFT in a pure state $|\psi\rangle$, let the system time evolve, and ask to what extent the state of system can be well approximated by a thermal state (global thermalization) and to what extent a subsystem can be well approximated by a subsystem of a thermal system (local thermalization).

A unique feature of 2D CFTs is that they have an infinite symmetry algebra that creates new states $|\psi'\rangle \sim \sum \prod L_{-k_i}|\psi\rangle$ from $|\psi\rangle$. We would expect that these symmetries do not affect whether or not a system globally thermalizes, but it is not *a priori* clear in what way these symmetry generators affect local thermalization. The example of the rectangle state (which is related to the ground state by symmetries) shows that local thermalization can occur even in states that are descendants of the ground state: by restricting observations to a small interval on the rectangle, the geometry observed is effectively that of the infinite strip and therefore thermalization is observed. It would be quite interesting to develop a more quantitative theory explaining to what extent subsystems in states that are descendants of the ground state are approximately thermal. Given that the behavior of the systems of interest seems to be fixed by geometry and symmetries alone, such a quantitative description should be possible, and we hope to report on it elsewhere. In the meantime we will present

the holographic dual point of view.

In holography, states that are descendants of the ground state and that have a semiclassical gravitational dual are described by geometries that are diffeomorphic to global AdS_3. General descendants of the ground state are described by AdS_3 with many graviton excitations, and different semiclassical AdS_3 geometries correspond to various Virasoro coherent states. Diffeomorphisms that preserve a convenient Fefferman-Graham gauge choice act on AdS_3 as follows. We start with vacuum AdS with metric $ds^2 = (dw^2+dzd\bar{z})/w^2$, and perform the following coordinate transformation

$$w \to \frac{w\sqrt{\partial f \bar{\partial} \bar{f}}}{N}, \quad z \to f(z) - \frac{w^2}{2}\frac{\partial f \bar{\partial}^2 \bar{f}}{\bar{\partial}\bar{f} N}, \quad \bar{z} \to \bar{f}(\bar{z}) - \frac{w^2}{2}\frac{\bar{\partial}\bar{f}\partial^2 f}{\partial f N}, \tag{2.2.1}$$

where

$$N = 1 + \frac{w^2}{4}\frac{\partial^2 f \bar{\partial}^2 \bar{f}}{\partial f \bar{\partial}\bar{f}}. \tag{2.2.2}$$

We then obtain a metric of the form

$$ds^2 = \frac{dw^2 + dzd\bar{z}}{w^2} - \frac{6}{c}T(z)dz^2 - \frac{6}{c}\bar{T}(\bar{z})d\bar{z}^2 + \frac{36}{c^2}w^2 T(z)\bar{T}(\bar{z})dzd\bar{z} \tag{2.2.3}$$

where

$$T(z) = \frac{c}{12}\{f, z\}, \quad \bar{T}(\bar{z}) = \frac{c}{12}\{\bar{f}, \bar{z}\}, \tag{2.2.4}$$

and the Schwarzian derivative is as usual

$$\{f, z\} = \frac{\partial^3 f}{\partial f} - \frac{3}{2}\left(\frac{\partial^2 f}{\partial f}\right)^2. \tag{2.2.5}$$

If we restrict to an interval where $T(z)$ and $\bar{T}(\bar{z})$ are approximately constant, then the bulk geometry in the neighborhood of that interval will be close to the BTZ geometry[5] [69], and correlation functions computed there are approximately the same as the finite temperature correlation functions obtained from the BTZ geometry. Thus in order to obtain local

[5]The metric 2.2.3 corresponds to the metric of [69] under the variable change $\rho = -\ln w$ and upon setting $c = \frac{3\ell}{2G}$.

thermalization we should apply a diffeomorphism that produces a locally constant $T(z)$ and $\bar{T}(\bar{z})$. An example of such a diffeomorphism is one that is locally approximately an exponential $f(z) = \exp(\alpha z)$ as this has a constant Schwarzian derivative. This is not too surprising as an exponential map essentially produces a local version of the Unruh effect whereby accelerated observers observe a thermal state.

Globally, then, these diffeomorphisms produce what would appear as a local concentration of energy-density repeatedly oscillating (due to the global periodic time-dependence) in AdS, but that does not form a black hole even at arbitrarily late times. It is therefore clear that diffeomorphisms alone, absent additional energy injections into AdS, never produce global thermalization. This leads to an interesting reverse question: given the expectation values of $T(z)$ and $\bar{T}(\bar{z})$ in some state, is it possible to come up with a diagnostic for whether or not the dual description of this state involves a black hole? In order to find such a diagnostic, we need to make sure that our diagnostic is not sensitive to diffeomorphisms, as the question of whether or not there is a black hole is clearly diffeomorphism invariant.

Perhaps the simplest way to analyze this problem is to find a diffeomorphism that makes $T(z)$ and $\bar{T}(\bar{z})$ constant and to read off the relevant constant values[6]. If both are larger than 0 in the planar case (or larger than $c/24$ in the global case) then the dual description can possibly involve a black hole, whereas for smaller values this is impossible and the system does not exhibit global thermalization. Note that this is a necessary, not a sufficient, condition for the existence of a black hole, as a large amount of dilute matter could also produce the relevant energy densities without there being a black hole.

The Chern-Simons description of three-dimensional gravity suggests a different way to do this computation. Diffeomorophisms act as gauge transformations on the $\mathrm{SL}(2,\mathbb{R})$ gauge

[6]There is a subtlety here, as such a diffeomorphism may not always exist. As nicely reviewed in [70], one can classify the $T(z)$ that are inequivalent under diffeomorphisms of the circle, which is the same as the classification of the so-called Virasoro coadjoint orbits. Besides the orbits which contain a point with constant $T(z)$, there are several other orbits, but all of these orbits except one have an energy L_0 which is unbounded from below and are therefore most likely unphysical. The one remaining orbit, labeled $\mathcal{P}_1^-$ in [70], has energy bounded from below, and its physical relevance (if any) is not clear to us. In any case, if we use the Chern-Simons description, and use $SL(2,\mathbb{R})$ gauge transformations instead of diffeomorphisms, we can always achieve constant T. We will ignore this subtlety in the remainder of this chapter and would like to thank Glenn Barnich for drawing our attention to this issue.

field

$$A = \begin{pmatrix} 0 & 1 \\ \frac{6}{c}T & 0 \end{pmatrix} \tag{2.2.6}$$

and therefore the relevant constant values of T can also be read off from the Wilson loop [71]

$$\cosh \frac{6}{c} T_{const} = \frac{1}{2} \mathrm{Tr} P \exp \oint A dx. \tag{2.2.7}$$

One can think of the coordinates that yield constant values for $T(z)$ as the AdS_3 analogue of the "center of mass" frame.

As a side remark, the geometries (2.2.3) have recently been used to study gravitational hair for black holes, see e.g. [72–74], with $T(z)$ and $\bar{T}(\bar{z})$ playing the role of the gravitational hair. From the Chern-Simons point of view the only gauge-invariant observables in the theory are the Wilson loops (2.2.7), which commute with all the Virasoro generators and which can be viewed as a Casimir for the Virasoro generators. These measure the invariant mass and angular momentum of the black hole. By contrast, there is no gauge-invariant observable in Chern-Simons theory that measures the gravitational hair away from the boundary of AdS or near the horizon of the black hole. In particular, there is no observable in the interior of AdS in Chern-Simons theory that would allow one to detect the gravitational hair, suggesting that the hair has nothing to do with the degrees of freedom making up the black hole[7].

The above considerations are meant to illustrate that while the stress tensor alone may provide some indication of thermalization, it is not a sufficiently sensitive diagnostic. This can be further motivated by observing that in theories with holographic duals the stress tensor only captures the behavior of the metric near the boundary of AdS. The analysis of physics deep inside the bulk, including whether or not a black hole is present, in general requires a knowledge of the expectation values of other operators in the theory as well.

More generally, in arbitrary CFTs the expectation values of all the higher conserved charges can be rendered constant by acting with more complicated Virasoro symmetries

[7] We would like to thank the participants of the Workshop on Topics in Three Dimensional Gravity (ICTP, Trieste) for useful discussions of these points.

(beyond diffeomorphisms). However, these higher conserved charges do not appear to play an important role in AdS/CFT, which we shall see for the case of 2+1 dimensions in Sec. 2.5.

Finally, we note that the holographic bulk geometries obtained via (2.2.3) are dual to conformal transformations of the CFT on the full plane. In order to apply this approach to find the holographic dual of arbitrary bounded subsets of this CFT, i.e. BCFTs, it is necessary to equip this description with an appropriately-chosen extension of the boundary of the CFT to the bulk - a bulk brane that bounds the spacetime region dual to this BCFT in the spirit of the AdS/BCFT correspondence of [75, 76]. Applying (2.2.3) to such setups in order to describe holographically a large class of holographic duals to BCFTs is an interesting direction that we leave to future work. Importantly, however, the presence of such a bulk brane is not expected to affect the local bulk physics in the deep interior (far away from the brane) of this spacetime, so that the above statements regarding local thermalization should carry over in the BCFT regime as well so long as the subsystem considered is sufficiently far from the boundary endpoints of the CFT.

2.3 Non-equilibrium behavior from CFT boundary states

The setup underlying the CFT non-equilibrium dynamics approaches of [51–57] and the work presented in Chapter 3 of this thesis – and which lends a physical interpretation to the strip and rectangle states – is that of the Calabrese and Cardy (CC) boundary state model for non-equilibrium evolution in CFTs [51, 52]. This boundary state setup relies on the existence of a well-defined analytic continuation from Lorentzian to Euclidean time in the system. This allows an initial state of the system $|\psi_0\rangle$ to be described as a Euclidean boundary state $|B\rangle$. The system is taken to have a Hamiltonian H, and the initial state $|\psi_0\rangle$ is assumed to be an eigenstate of a different Hamiltonian H_0. Conformal boundary states are in fact non-normalizable, and in practice the quench is taken to be from a gapped Hamiltonian, so that the actual Euclidean boundary state is given by a state that is irrelevantly perturbed

from the conformal boundary state $|B\rangle$; by convention it is taken to be

$$|\psi_0\rangle_E \propto e^{-\tau_0 H} |B\rangle \,, \tag{2.3.1}$$

where τ_0 is on the order of the correlation length of the gapped Hamiltonian H_0. We note that $H \propto \int T_{tt} dx$, where $T_{tt} \propto T(z) + \bar{T}(\bar{z})$, and in general additional irrelevant operators are expected to contribute. More general forms of boundary states where additional conserved charges or boundary operators are introduced in the exponential and act on the conformal boundary state were considered in [60–62]. The restriction to T_{tt} in (2.3.1) was motivated in [55] by noting that T_{tt} is often the leading irrelevant operator acting on the boundary state, and here we restrict our analysis to this form.

At $t = 0$ the system is put in the state $|\psi_0\rangle$, and it is thereafter allowed to evolve unitarily as $e^{-iHt} |\psi_0\rangle$. Correlation functions of observables $\mathcal{O}(t, x)$ are therefore given by

$$\langle \mathcal{O}(t,x) \rangle = \left\langle \psi_0 \left| e^{iHt} \mathcal{O}(x) e^{-iHt} \right| \psi_0 \right\rangle ,$$

and upon analytic continuation to Euclidean time can be computed via a path integral over a strip, of width $2\tau_0$, with the operator $\mathcal{O}$ inserted at $\tau = \tau_0$ and analytically continued as $\tau \to \tau_0 + it$.

In a 2D CFT, where the strip of width $2\tau_0$ can be conformally mapped to the upper-half plane (UHP) as $w \to z(w) = e^{\frac{\pi}{2\tau_0} w}$, correlation functions in this setup can simply be computed by conformal transformations from the correlation functions of a boundary CFT (BCFT) on the UHP. This setup was used by CC to show that one-point functions decay exponentially for $t \gg \tau_0$ and to compute the time evolution of correlations between two primary operators (via the two-point function).

Since the restriction of the CFT to the UHP reduces the symmetry group of the CFT, boundary conditions must be enforced at the interface such that the conformal symmetry group is retained under conformal maps from the UHP. These are given by the condition

that there should be no energy or momentum flow across the boundary, $T_{xy}\big|_{y=0} = 0$, or

$$T(z) = \bar{T}(\bar{z})\big|_{z=\bar{z}}\,. \tag{2.3.2}$$

In the presence of additional symmetries in the CFT, boundary conditions that retain these symmetries may be imposed; however, the specification of the BCFT alone does not require the boundary to respect these additional symmetries.

The implication of this conformal boundary condition is that the holomorphic and anti-holomorphic sectors of the CFT are no longer independent. In particular, n-point bulk correlators $\left\langle \phi_{h_1,\bar{h}_1}(z_1,\bar{z}_1)\,\phi_{h_2,\bar{h}_2}(z_2,\bar{z}_2)\,...\phi_{h_n,\bar{h}_n}(z_n,\bar{z}_n)\right\rangle$ on the upper-half plane obey the same Ward identities as the formal $2n$-point correlators of holomorphic fields on the full plane [77],

$$\left\langle \phi_{h_1}(z_1)\,\phi_{\bar{h}_1}(z_1^*)\,\phi_{h_2}(z_2)\,\phi_{\bar{h}_2}(z_2^*)\,...\phi_{h_n}(z_n)\,\phi_{\bar{h}_n}(z_n^*)\right\rangle .$$

The presence of the boundary thus implies that, e.g., one-point functions of primary operators no longer vanish in general on the UHP and are determined by conformal invariance up to a constant to have the form $\left\langle \phi_{h,\bar{h}}(z,\bar{z})\right\rangle \sim (z-\bar{z})^{-2h}$ for $h=\bar{h}$.

The infinite conformal symmetry of 2D CFTs allows a boundary state defined on the upper-half plane to be mapped to an effectively unlimited range of bounded domains, with the strip only one particular example; as noted earlier, such mappings do not affect the thermal behavior of the system, and whether or not the system reaches a global thermal state is invariant under these transformations. Consequently, the out-of-equilibrium behavior of a system from a particular boundary state can be investigated in any of the conformally-equivalent boundary states. In the absence of additional operator insertions, these states are simple conformal mappings of the ground-state on the UHP and do not exhibit global thermalization. As noted earlier, any of these boundary states can be mapped to the strip geometry, where the expectation value of the stress tensor is a constant Casimir value due to the vanishing of $\langle T(z)\rangle$ on the ground-state on the UHP. The simplest modifications of the boundary states that potentially exhibit global thermalization are those obtained by

local operator insertions. As we show below, to diagnose thermalization of such systems, it is necessary to consider more refined observables. If additional operators are inserted on the boundary of the domain, conformal mappings do not affect the nature of these fields as boundary fields, since the boundary of a given system (e.g. the x-axis on the UHP) is mapped to the boundary of the conformally transformed system.

2.3.1 Revivals in finite-length systems

The finite-length equivalent of the CC setup is a boundary state defined on a strip with spatial boundaries. Such bounded domains, with a vast array of differently-shaped boundaries, can be obtained by Schwarz-Christoffel maps [78] from the UHP to bounded polygonal geometries. These transformations map a set of designated prevertices on the real line of the complex plane to the vertices of a new polygonal domain, with the real line mapped to the boundary of the domain. In particular, we can consider the map to a rectangle. For

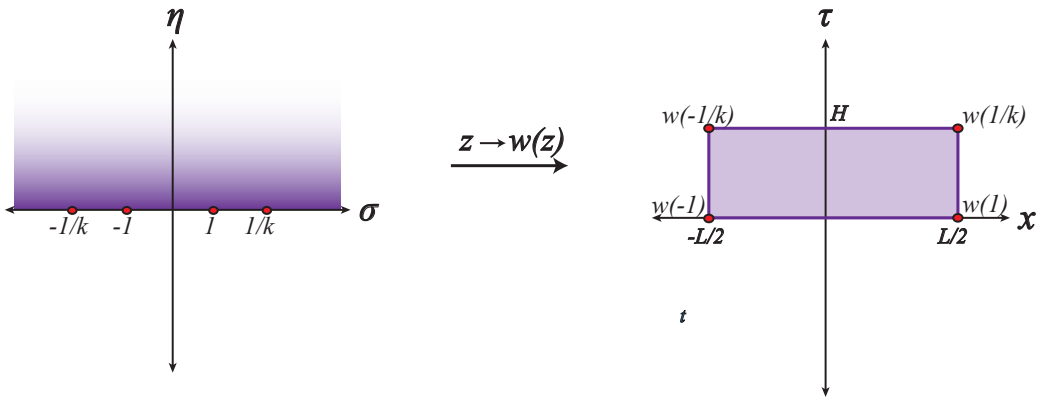

Figure 2.1: The Schwarz-Christoffel conformal transformation that maps the UHP with designated prevertices to a rectangle.

prevertices at $x = \pm 1, \pm\frac{1}{k}$, the general form of the map $z \to f(z) = w$ to the rectangle is given by the integral expression

$$w(z) = A \int_0^z \frac{d\zeta}{(\zeta-1)^{\frac{1}{2}}(\zeta+1)^{\frac{1}{2}}\left(\zeta-\frac{1}{k}\right)^{\frac{1}{2}}\left(\zeta+\frac{1}{k}\right)^{\frac{1}{2}}}$$

where A is a constant that can be freely chosen. With a choice of $A = -\frac{L}{2kK_1(k^2)}$, where $K_1(k^2)$ is the complete elliptic integral of the first kind and $k \in [0,1]$, $w(z)$ is given by

$$z \to w(z) = \frac{L}{2K_1(k^2)} F\left(\arcsin z, k^2\right), \tag{2.3.3}$$

an elliptic integral of the first kind, and maps the UHP to a rectangle with vertices at $\left(\pm\frac{L}{2}, 0\right)$ and $\left(\pm\frac{L}{2}, H\right)$, where $H = \frac{K_1\left(1-k^2\right)}{2K_1(k^2)}$ is the height of the rectangle (Fig. 2.1). The geometry of the rectangle is fully determined by the ratio L/H. The limit of $k \to 1$ corresponds to the zero-height rectangle, and in this limit the system appears infinite in length. The limit of $k \to 0$ corresponds to the semi-infinite strip with width L.

The inverse map from the rectangle to the UHP is given by the elliptic Jacobi function

$$w \to z(w) = \mathrm{sn}\left(\frac{2K_1(k^2)}{L} w, k^2\right), \tag{2.3.4}$$

which is periodic in its argument as

$$\mathrm{sn}\left(\frac{2K_1(k^2)}{L}\left(w + mL + 2inHL\right), k^2\right) = (-1)^m \,\mathrm{sn}\left(\frac{2K_1(k^2)}{L} w, k^2\right).$$

We will denote the complex coordinate on the rectangle by $w = x + i\tau$, with τ the Euclidean time direction along the height of the rectangle and x the direction along its width. Observables in this geometry are inserted on the rectangle and analytically continued to Lorentzian times as $\tau \to \frac{H}{2} + it$, where t denotes the Lorentzian time coordinate. As a result, (2.3.4) is periodic in Lorentzian time with period equal to $2L$. Since correlation functions on the rectangle are calculated from their counterparts on the UHP, every argument z of a Lorentzian operator assumes an inherent periodicity; e.g. one-point functions of primary operators of conformal dimension h in the conformal mapping of the UHP ground-state are given by

$$\langle \mathcal{O}(t,x) \rangle \sim \left(\frac{dz(w)}{dw}\frac{d\bar{z}(\bar{w})}{d\bar{w}}\right)^h \left(z(w) - \bar{z}(\bar{w})\right)^{-2h} \Bigg|_{\substack{w \to x - t + iH/2 \\ \bar{w} \to x + t - iH/2}} \tag{2.3.5}$$

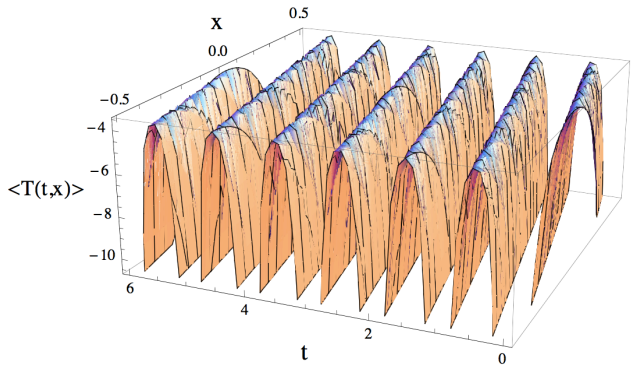

(a) Profile of the expectation value of the holomorphic stress tensor $T(t, x)$ across the rectangle.

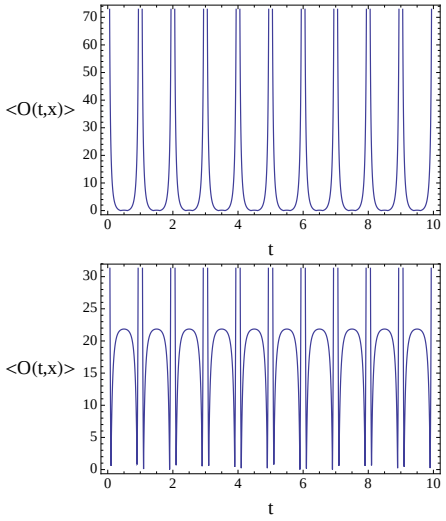

(b) One-point functions $\langle \mathcal{O}(t, x) \rangle$ at sample points $x = 0.1$ (top) and $x = 0.4$ (bottom).

Figure 2.2: Periodicity in observables in the rectangle ground state. Plot parameters are $k = 0.5$ and $L = 1$.

and the stress tensor is given by

$$\langle T(t, x) \rangle = \frac{c}{12} \{z(w), w\}, \tag{2.3.6}$$

where c is the central charge and $\{z(w), w\} = \frac{z^{(3)}(w)}{z'(w)} - \frac{3}{2} \left(\frac{z^{(2)}(w)}{z'(w)} \right)^2$ is the Schwarzian derivative. The periodicity of (2.3.5) and (2.3.6) in Lorentzian time is therefore evident (Fig. 2.2). The periodicity of these observables as resulting from the nature of the conformal mapping and the implication that the rectangle state features non-thermal behavior was also pointed out in [56].

As we reviewed, conformal transformations of the vacuum state on the upper-half plane do not thermalize, but one might expect that perturbations of this boundary state should eliminate the non-thermal behavior. Rectangle states perturbed by operator insertions in $c = 1$ CFT were first considered in a somewhat different context in the work presented in the next chapter of this thesis. The setup described in that chapter ascribes a physical

interpretation to these types of perturbed states by drawing an analogy with the experimental system of the "Quantum Newton's Cradle" experiment [43]. Below we investigate how the time evolution of similar states is affected by the spectrum of the CFT (rational vs. non-rational), and whether a given system may exhibit periodic revivals at asymptotically late times. Recall that, as was pointed out in Sec. 2.2, the expectation value of the stress tensor itself is in general an insufficient diagnostic of thermalization. In particular, in a state perturbed by Euclidean-time operator insertions $\mathcal{O}_i$ with conformal dimensions h_i, the time dependence in the expectation value of the stress tensor is determined purely by conformal invariance:

$$\left\langle T(z) \prod_i \mathcal{O}_i(\zeta_i) \right\rangle = \sum_i \left[\frac{h_i}{(z_i - \zeta_i)^2} + \frac{\partial_{\zeta_i}}{z_i - \zeta_i} \right] \left\langle \prod_i \mathcal{O}_i(\zeta_i) \right\rangle ,$$

since only the stress tensor coordinate z is continued to Lorentzian time. As a result, the time evolution of this expectation value is qualitatively identical regardless of the spectrum of the CFT and cannot be used to resolve any potential differences for CFTs with $c < c_{\text{crit}}$ versus those with $c > c_{\text{crit}}$. In the next section we therefore probe perturbations of boundary states using one-point functions of generic operators that do not correspond to conserved currents, focusing on the different behaviors of rational vs. non-rational CFTs.

2.4 Operator spectrum dependence of thermalization

In this section we consider expectation values of primary operators in perturbed states. The simplest perturbed states are those produced by a path integral over a suitable Euclidean domain with a single operator insertion on the boundary of the domain. The expectation value of a single operator in such a state will then be given by the analytic continuation of a three-point function with two operators on the boundary (one for the in-state and one for the out-state) and one operator in the interior. Conformal invariance fixes the form of these three-point functions up to a single unknown function of a suitable cross-ratio. Even without knowing the explicit form of this function (which would involve knowledge of the structure constants and conformal blocks of the theory) one can already see a qualitative change in the

behavior of the part of the three-point function that is determined by conformal invariance (and that we henceforth refer to as the "universal" part of the correlation function) as one moves from rational to non-rational theories. In particular, exact periodicity of the expectation value appears to be lost[8], in agreement with the picture that rational theories should not display global thermalization and irrational theories should. However, without more detailed knowledge of the exact correlation function, it is not possible to see the destructive interference which leads to exponential decay to the thermal value of one-point functions, and, while suggestive, our analysis is by no means to be taken as a proof of thermalization in irrational CFTs.

2.4.1 General setup

It is in principle possible to consider very general classes of states created by a path integral over arbitrary bounded domains with a particular boundary state on the boundary and arbitrary insertions of operators in the interior of the domain and on its boundary. Even in the absence of operator insertions, correlation functions computed in states of this type are in general time dependent. As we discussed in section 2.2, the time dependence in the expectation value of the energy momentum tensor can in general be removed by applying a suitable diffeomorphism, and we will therefore focus on the geometries with a time-independent expectation value for the energy-momentum tensor, which are infinite strip geometries.

We consider an infinite Euclidean strip of the form $w = x + i\tau$ with $(x, \tau) \in [0, 2L] \times (-\infty, \infty)$, which can be mapped to the upper half plane via the map $z(w) = e^{\frac{\pi i w}{2L}}$, with z the coordinate on the upper half plane. Such an infinite strip can be interpreted in two different ways, either as providing an in- and an out-state on the theory on a finite interval of length $2L$, but also as providing an in- and an out-state on an infinite spatial interval. In the latter case, the roles of space and time should be exchanged[9], so that Euclidean time

[8] To see this, as we discuss below, we in fact need to consider linear superpositions of states obtained by operator insertions.

[9] This is the strip state of CC [51, 52].

runs from 0 to $2L$ and space from $-\infty$ to $+\infty$. Moreover, the relevant analytic continuation to Lorentzian time is $w = x - t$ in the first case, and $w = L + it + i\tau$ in the second case. We will mostly take the point of view of the finite strip in what follows, but the infinite strip can be treated in exactly the same way.

We insert n_1 boundary operators $\mathcal{O}_B$ on the left boundary of the strip at $w_a = i\tau_a$, and n_2 bulk operators $\mathcal{O}$ at positions $w_p = x_p + i\tau_p$. For simplicity, we will not insert any operators on the right boundary of the strip, but this is a straightforward generalization. In order to be able to interpret the boundary insertions as corresponding to an in- and an out- state, the boundary operators should be distributed symmetrically around $\tau = 0$. However, if we are interested in studying linear superpositions of states, we should also consider asymmetric distributions of operators.

2.4.2 Periodicity in correlation functions

The general form of the correlation function can be obtained by mapping it to the upper-half plane and using $SL(2,\mathbb{R})$ Ward identities. To write the result we denote

$$(\xi_1, \ldots, \xi_N) = (\{z_a(w_a)\}, \{z_p(w_p)\}, \{\bar{z}_p(\bar{w}_p)\}), \quad N = n_1 + 2n_2, \tag{2.4.1}$$

in term of which the correlator is, up to an overall constant factor,

$$\left\langle \prod_a \mathcal{O}_{B,a}(w_a) \prod_j \mathcal{O}_p(w_p) \right\rangle = \prod_i^N \xi_i^{h_i} F\left(\frac{\xi_{ij}\xi_{kl}}{\xi_{ik}\xi_{jl}}\right) \prod_{i<j} \xi_{ij}^{\frac{2}{N-2}(h_\Sigma/(N-1)-h_i-h_j)} \tag{2.4.2}$$

where $h_\Sigma = \sum h_i$ and $\xi_{ij} = \xi_i - \xi_j$, and F a function of cross ratios. Note that the conformal dimensions h_i refer to both those of the bulk operator, h, $\bar{h}$ as well as those of the boundary operators, h_B. The prefactor $\prod \xi_i^{h_i}$ is due to the map from the strip to the upper-half plane and includes contributions from the coordinates of all operators[10]. It can be absorbed in a

[10]This prefactor is given by $\prod_i \left(\frac{dw_i(z_i)}{dz_i}\right)^{-h_i}$, which on the strip becomes $\prod_i (z_i(w_i))^{h_i}$ up to a constant factor.

nice way in the rest of the expression by defining

$$\tilde{\xi}_{ij} = \frac{\xi_i - \xi_j}{\sqrt{\xi_i \xi_j}} = 2i \sin\left[\frac{\pi}{4L}(w_i - w_j)\right], \tag{2.4.3}$$

in terms of which the general correlator is of the form

$$\left\langle \prod_a \mathcal{O}_{B,a}(w_a) \prod_p \mathcal{O}_p(w_p) \right\rangle = F\left(\frac{\tilde{\xi}_{ij}\tilde{\xi}_{kl}}{\tilde{\xi}_{ik}\tilde{\xi}_{jl}}\right) \prod_{i<j} \tilde{\xi}_{ij}^{\frac{2}{N-2}(h_\Sigma/(N-1)-h_i-h_j)}. \tag{2.4.4}$$

Note that because the exponential map that we employ here has an explicit dependence on i in it,

$$(w_1, \ldots, w_N) = (\{w_a\}, \{w_p\}, \{-\bar{w}_p\}). \tag{2.4.5}$$

Upon analytic continuation of a particular bulk operator to Lorentzian time, $w \to x - t$, it is clear from (2.4.3) that the correlation function will contain contributions of the form $f(t) = (\sin(\frac{\pi}{4L}(t-c)))^s$, with complex c, which might appear to be periodic with period of at most $8L$, except that s is in general not an integer and $f(t)$ has to be defined through analytic continuation. For complex c, the function $z(t) = \sin(\frac{\pi}{4L}(t-c))$ follows a contour around the origin in the complex plane that we can write as $z(t) = r(t)e^{i\phi(t)}$, with both $r(t)$ and $\phi(t)$ periodic with period $8L$. The analytic continuation of $z(t)^s$ is clearly $r(t)^s e^{is\phi(t)}$, which is now no longer periodic unless s is rational. This is an indication that the time-dependence of correlation functions in rational theories will have special properties and tend to be periodic.

We will consider pure states of the form $\sum_i |\psi_i\rangle$ where each $|\psi_i\rangle$ is obtained through a path integral on the half-strip with suitable operator insertions. Expectation values of bulk operators in such states require us to compute matrix elements $\langle\psi_i| \prod_k \mathcal{O}_k |\psi_j\rangle$.

We first focus on the diagonal matrix elements. For those, it turns out that the universal part of the correlation function will always be periodic. To see this, we observe that the

correlation function will contain a product of terms of the form

$$\left[\sin\left(\frac{\pi}{4L}(t-x+i\tau_0)\right)\sin\left(\frac{\pi}{4L}(t-x-i\tau_0)\right)\right]^s, \tag{2.4.6}$$

which can be rewritten as the purely real expression

$$2^{-s}\left[\cosh\left(\frac{\pi}{2L}\tau_0\right)-\cos\left(\frac{\pi}{2L}(t-x)\right)\right]^s, \tag{2.4.7}$$

which is well-defined with period $4L$.

Any possible breakdown of periodicity in diagonal matrix elements therefore has to originate from the function F of the cross-ratios that appears in the correlation function as well. Unfortunately, it is much more difficult to analyze this function in general. If we take the simplest example with two boundary insertions at $\pm i\tau_0$ and one bulk operator, the cross-ratio (after analytic continuation) takes the form

$$y=\frac{\tilde{\xi}_{w,\bar{w}}\tilde{\xi}_{w_1,w_2}}{\tilde{\xi}_{w,w_1}\tilde{\xi}_{\bar{w},w_2}}=\frac{\sin\left[\frac{\pi}{2L}x\right]\sin\left[\frac{\pi i}{2L}\tau_0\right]}{\sin\left[\frac{\pi}{4L}(t-x-i\tau_0)\right]\sin\left[\frac{\pi}{4L}(t+x+i\tau_0)\right]}. \tag{2.4.8}$$

We see that y does not go around one of the singularities at $y=0,1,\infty$ and that therefore the unknown function of the cross ratio will remain periodic[11] with period $4L$. Finally, for boundary operators inserted at $\pm\infty$ ($\tau_0\to\infty$), the cross ratio becomes time independent:

$$y=e^{\frac{\pi i x}{L}}-1, \tag{2.4.9}$$

so that no decay in time can be seen for such operator placement. There may be an argument as to why diagonal matrix elements always remain periodic based on the symmetry $\tau\leftrightarrow-\tau$, but we have not explored this in detail.

Off-diagonal matrix elements, on the other hand, appear to lose their periodicity in

[11] We can also see this by observing that the denominator of (2.4.8) can be expanded as $\frac{1}{2}\left(\left(a^2+b^2\right)\cos\left(\frac{\pi x}{2L}\right)-2iab\sin\left(\frac{\pi x}{2L}\right)-\cos\left(\frac{\pi t}{2L}\right)\right)$ where $a=\cosh\left(\frac{\pi\tau_0}{4L}\right)$ and $b=\sinh\left(\frac{\pi\tau_0}{4L}\right)$, so that it is given by the sum of a real time-periodic and a complex time-independent function.

general. This is already clear at the level of the universal part of the correlation function, where factors of the form $[\sin\frac{\pi}{4L}(t-c))]^s$, $c = x + i\tau_0$, are no longer paired with factors $[\sin\frac{\pi}{4L}(t-c^*)]^s$ as in (2.4.6), resulting in an expression consisting of powers of periodic functions that are complex in the time argument. If s is rational, these factors will remain periodic but with a longer period, but if s is irrational periodicity is lost altogether. Of course, for a complete analysis it is necessary to also consider the in general unknown functions of the cross-ratios[12]. The analytic properties of correlation functions, and more generally the analytic properties of conformal blocks, are typically closely related to the braiding and fusion properties of the theory. For rational theories the space of conformal blocks form finite dimensional representations under fusion and braiding, which in turn is closely related to the periodicity of correlation functions[13]. One would therefore expect to see periodicity in the case of rational theories, and a breakdown of periodicity in irrational theories. As we have explained, we already see signs of this breakdown in simple correlation functions, and it would be interesting to explore this further.

2.5 The holographic dual of the generalized Gibbs ensemble

As mentioned in the introduction, conformal field theories have a large number of conserved currents. For example, any polynomial made out of the stress tensor $T(z)$ and its derivatives is a conserved current. Similarly, if there are additional higher spin currents, any polynomial involving those leads to conserved currents as well. Given such large sets of conserved currents, one can ask what the maximal set of conserved and commuting charges is. For the case of the Virasoro algebra, there exists a conserved current, unique up to total derivatives,

[12] One can easily check in examples of $c = 1$ theories where correlation functions of primaries can be explicitly written down that these conclusions indeed hold for the full correlation functions: for rational $c = 1$ theories periodicity is maintained, while for irrational $c = 1$ theories periodicity is lost. (Note that periodicity is maintained if we take as our operators to be $\partial\phi$ or $\bar{\partial}\phi$, but since these operators correspond to conserved currents they should not be considered for diagnosing whether the system experiences revivals as previously explained.) Because $c = 1$ theories are exactly solvable we do expect these theories to be described by a suitable generalized Gibbs ensemble at late times under generic perturbation, see [61, 62].

[13] which we already knew to be periodic in time anyway in view of the straightforward argument in the introduction.

whose zero modes all commute. In the semi-classical case, where we replace OPEs by Poisson brackets, the construction of these conserved currents and corresponding conserved charges is captured by the KdV hierarchy. The KdV hierarchy does in fact also describe the flows generated by the complete set of commuting conserved charges. A conformal field theory contains a quantum deformation of the KdV hierarchy, the quantum KdV hierarchy, see [59].

Since the stress tensor is a single trace operator, adding polynomials of the stress tensor and its derivatives with chemical potentials to the action (in order to describe a generalized Gibbs ensemble) corresponds to multitrace deformations in the CFT. Multitrace deformations both in pure gravity as well as in its higher spin extensions can be conveniently studied in the Chern-Simons formulation, and a detailed discussion will appear elsewhere [79]. Here we simply summarize a few key ingredients using the notation from [80].

In general, if we add a multitrace deformation of the form $\int \Omega \equiv \sum_i \nu_i F_i(W_s)$, with the ν_i chemical potentials which we will take to be constant, and $F(W_s)$ polynomials in the higher spin fields and their derivatives, all we need in Chern-Simons theory is a boundary term of the form

$$I_B^{(E)} = -\frac{k_{cs}}{2\pi} \int_{\partial M} d^2z \, \mathrm{Tr} \left[(a_z + a_{\bar{z}}) a_{\bar{z}} - 2\Omega \right] \tag{2.5.1}$$

plus a similar result for the right movers. Moreover, whereas $a_{\bar{z}}$ usually contains the sources μ_s for the higher spin fields W_s, we now need to replace these sources μ_s by $\partial\Omega/\partial W_s$. We therefore in general have a non-linear relation between the normalizable and non-normalizable modes, which is typical for multitrace deformations [81,82]. The variation of the on-shell action consisting of standard Chern-Simons theory plus the boundary term can be written as

$$\delta(I_{CS}^{(E)} + I_B^{(E)}) = \frac{k_{cs}}{\pi} \int_{\partial M} d^2z \, \mathrm{Tr} \sum_i \delta\nu_i F_i(W_s), \tag{2.5.2}$$

which indeed has the right structure.

Although we could continue our discussion in the language of Chern-Simons theory, from the above it should be clear that the bulk field equations are not modified, and that once we restrict to translationally invariant solutions, in the bulk the solution looks just like the

BTZ black hole and its higher spin generalizations. This is also immediately the main point of this section: classically there are no hairy black holes corresponding to the generalized Gibbs ensemble, the bulk geometry is still the BTZ geometry. The free energy or partition function is however different from that of the usual BTZ black hole, because of the additional boundary terms that one needs. In fact, looking carefully at the Chern-Simons formulation, one finds that the contribution of the left-movers to the partition function for the pure gravity case with a deformation

$$\int d\sigma \sum_i \mu_i F_i(T)$$

is equal to

$$Z = \mathrm{Tr}(e^{-\int d\sigma \sum_i \mu_i F_i(T)}) = e^{2\pi\sqrt{\frac{c}{6}L_0} - \sum_i 2\pi\mu_i F_i(L_0)} \,|_{saddle}\,. \tag{2.5.3}$$

Here, saddle means that we have to extremize the right hand side with respect to L_0, and the answer therefore looks like a generalized Legendre transform of the expression of the black hole entropy. Here, because we restrict to translationally invariant solutions, all terms containing derivatives of T drop out of $F_i(T)$, and these functionals become ordinary functions of the zero mode L_0. Thus, using the bulk gravitational description simplifies the GGE dramatically, the zero modes of the higher spin conserved currents are polynomials in terms of L_0 and no longer take on independent values.

It is straightforward to see that

$$\frac{\partial \log Z}{\partial \mu_i} = -2\pi F_i(L_0)|_{saddle}.$$

If we identify the $F_i(T)$ with the conserved charges of the KdV hierarchy, then the partition function is precisely a tau-function for the KdV hierarchy[14].

Though this is perhaps a somewhat trivial example of a tau-function, we can extend it to the case where T is no longer constant. For this we need to use the gauge invariant

[14]See, e.g. [83, 84] for the tau-function and [85] for the KdV hierarchy.

generalization of the entropy given by the appropriate Wilson line operator. The result is

$$Z = \mathrm{T}r(e^{-\int d\sigma \sum_i \mu_i F_i(T)}) = \exp\left\{ \frac{c}{6}\cosh^{-1}\frac{1}{2}\mathrm{T}rP\exp\oint \begin{pmatrix} 0 & 1 \\ \frac{6T}{c} & 0 \end{pmatrix} - \int d\sigma \sum_i \mu_i F_i(T) \right\}|_{saddle} \tag{2.5.4}$$

where now saddle means that we should find the saddle point of the expression on the right hand side for the functional $T(\sigma)$. This provides a more interesting class of tau-functions for the KdV hierarchy if the $F_i(T)$ are the corresponding charges, but at this level the $F_i(T)$ can in principle still be arbitrary, which is probably an artifact of the large c (or large k) limit. We expect that once we start quantizing Chern-Simons theory with matter we should see a more interesting structure emerge, and, in particular, we expect gravitational solutions that depend non-trivially on the chemical potentials μ_i. It would be interesting to explore the construction of such "black holes with quantum hair" in more detail.

Finally, we note that while it is tempting to assume a connection between the conserved charges considered here and the conserved charges that appear in studies of integrability in AdS/CFT, the latter are generically non-local and are supposed to already be relevant at the semi-classical level. Therefore, an obvious connection is lacking, but it would also be interesting to explore this in more detail, as would be the role that the various conserved charges can possibly play in studying geon solutions and instabilities of AdS.

2.6 Discussion

In this paper we studied some properties of the non-equilibrium behavior of 2D CFTs as well as the distinction between local and global thermalization. We provided arguments that there are no revivals in generic states in irrational theories, which one could take as an indication that the system thermalizes. To actually see thermalization probably requires one to choose very complicated initial states for which explicit computations rapidly become intractable. One-point functions of light probes in very complicated, heavy states can presumably be well-approximated by the light-light-heavy-heavy conformal block derived in [86], although

these computations have to our knowledge not been extended to a situation with boundaries. Ultimately this is just another illustration of the usual problem that we can either do explicit, weakly coupled computations where unitarity is manifest but thermalization difficult to see, or we can do strongly coupled (e.g. gravitational) computations where thermality is easy to see but manifest unitarity is lost.

We note that there has been much research in recent years, starting with [33, 34, 87, 88], into the possibility of time-periodic solutions in AdS that avoid collapse into a black hole; however, exact solutions involving stable oscillating matter known to exceed the BTZ black hole mass threshold (in AdS_3) and yet exhibiting revivals to $t \to \infty$ (undamped oscillations) have so far not been found. If such solutions do exist, they appear likely to occupy a very small phase space and/or involve considerable simplifications of the physical setup.

In a similar spirit, we have shown that the holographic dual of the generalized Gibbs ensemble is still a BTZ black hole. The GGE has been central to the discussion of 1+1-dimensional integrable systems away from a conformal fixed point. Such integrable field theories can be obtained as massive deformations of a CFT, and – at least in principle – the analysis that was carried out here could be applied to them via conformal perturbation theory, where transformations to a frame of constant stress tensor can still be applied at every order.

We note several additional avenues that are of interest in light of our findings. The holographic picture of Sec. 2.2 for diffeomorphisms of the CFT ground state can be used to generalize the AdS/BCFT setup of [75, 76] to arbitrary forms of boundary states by finding the appropriate bulk brane corresponding to the extension into the bulk of the dual BCFT's boundary. In particular, the holographic dual of the rectangle state can thus be found, and Lorentzian-time correlators from the corresponding initial state can be computed via a formalism such as [89, 90]. The holographic implementation of such a setup would likely be a useful tool in evaluating general non-equilibrium behavior in systems with boundaries, not only in classical AdS geometries, but also to $1/N$ corrections. Finally, we note that while in classical $SL(2,\mathbb{R})$ Chern-Simons theory expectation values of Wilson lines in different

representations are related to each other in a simple way, this is no longer the case in quantum Chern-Simons theory. It would be interesting to explore these quantum expectation values in more detail and establish their relationship to the quantum KdV hierarchy and the GGE at finite values of the central charge.

CHAPTER 3

Non-equilibrium behavior in 1+1 dimensions from CFT boundary states and the "Quantum Newton's Cradle" experiment

In this chapter, a framework is presented for investigating the response of conformally-invariant confined 1+1-dimensional systems to a quantum quench. While conformal invariance is generally destroyed in a global quantum quench, systems that can be described as or mapped to integrable deformations of a CFT may present special instances where a conformal field theory-based analysis could provide useful insight into the non-equilibrium dynamics. The connections between systems that are integrable and those that are conformally-invariant have been subject to ongoing investigation; in particular, certain integrable field theories can be obtained from massive deformations of particular models of conformal field theory (CFT) [91], rendering the understanding of thermalization within a CFT framework a potentially powerful tool for testing some of the ideas arising in the study of the connections between conformal invariance and integrability [59, 92, 93]. In principle, if it is known how a particular integrable model arises as a perturbation at a conformal fixed point, conformal perturbation theory (see, e.g., [94]) can be used to compute observables of the integrable theory up to arbitrary order. While this approach may often become computationally cumbersome beyond the lowest orders, it raises the question of whether out-of-equilibrium analyses of certain CFTs may shed light on the post-quench behavior of related integrable models. We investigate this possibility by considering a quench analogous to that of the "Quantum Newton's Cradle" experiment [43] and demonstrating qualitative agreement between observables

derived in the CFT framework and those of the experimental system. We propose that this agreement may be a feature of the proximity of the experimental system to an integrable deformation of a $c = 1$ CFT.

Much of the discussion of non-thermalization and integrability in 1+1 dimensions in the past decade has been motivated by the 2006 "Quantum Newton's Cradle" experiment [43] at Pennsylvania State University. In that experiment, an effectively one-dimensional system of interacting harmonically-confined bosons was split into two oppositely-moving momentum groups. Following this quench, the system failed to demonstrate any apparent thermalization within experimental time scales. While some experimental effects, such as the presence of a confining trapping potential in the setup, may introduce weak integrability-breaking effects, the system is believed to be well-described by the integrable Lieb-Liniger model [95] of delta-interacting bosons, and the failure of the experimental system to thermalize has been attributed to the integrability of this model.

To motivate the relation to the CFT picture, we note that the non-relativistic Lieb-Liniger model can be exactly mapped to the relativistic sinh-Gordon model in an appropriate limit. In particular, under this mapping the S-matrix and Lagrangian of the two models coincide [96,97]. The sinh-Gordon model is a massive integrable deformation of a free scalar field Lagrangian, and correlation functions in this model can in principle be computed order-by-order in a conformal perturbation expansion.

By constructing a quench in the CFT boundary state model (see Chapter 2) that we argue is analogous to that performed in the experiment, we show that the "Quantum Newton's Cradle" system exhibits the behavior characteristic of a conformally-invariant system. We proceed as if this system were a $c = 1$ CFT, which is an accurate effective description of the Lieb-Liniger model in the limit of either low momenta or hard-core boson interactions (the latter which map to free fermions [98]). This amounts to neglecting higher order terms in a perturbative expansion of correlation functions of the sinh-Gordon model and hence its non-relativistic Lieb-Liniger limit. An important issue when truncating such a perturbative expansion is whether higher-order perturbative effects, which may not qualitatively change

the behavior in equilibrium, could have significant effect in a non-equilibrium setting on the asymptotic (long-time) behavior of observables. As we show, this does not appear to be the case in a qualitative analysis; we comment on this and suggest how a quantitative analysis may be performed in order to detect potential deviations.

In the free boson CFT analyzed here, the harmonic confinement of the system implies that (up to an overall rescaling) there is a full equivalence up to a phase lag of half the system's size between the position-space energy density expectation value (given by $\langle T_{tt} \rangle$) and the momentum-space expectation value. The latter is the CFT observable corresponding to the momentum distributions observed in the experiment. Although the experimental setup was in principle not limited to the low momenta or hard-core interactions regimes, we show that the experimental momentum distributions and this CFT observable qualitatively agree.

3.1 Implementation of confinement through the rectangle state

To make contact with the realistic system we take the system to be on a finite interval and employ the rectangle state discussed in Chapter 2. To obtain regulated expressions we will transform the right-half plane to the rectangle (rather than the upper-half plane as in (2.3.3)), using the mapping employed in [56] and given by the elliptic Jacobi function[1]

$$w \to z(w) = \mathrm{sc}\left(\frac{K_1(k)}{L}\left(w + \frac{L}{2}\right), k\right). \tag{3.1.1}$$

where k is the elliptic modulus, $k \in [0,1]$ and $K_1(...)$ is the complete elliptic integral of the first kind. Its inverse is a Schwarz-Christoffel transformation [78] given by the elliptic integral of the first kind

$$w(z) = \frac{L}{K_1(k)} F\left(\tan^{-1}(z), k\right) - \frac{L}{2}$$

and that maps a set of designated points $y = \pm 1, \pm 1/\sqrt{1-k}$ on the imaginary ($x = 0$) axis to the vertices of a rectangle as shown in Fig. 3.1 with height $2\tau_0 = 2K_1\left(\sqrt{1-k}\right)/K_1(k)$,

[1] The modification by an additive constant here from [56] centers the resulting rectangle on the origin of the transformed coordinates.

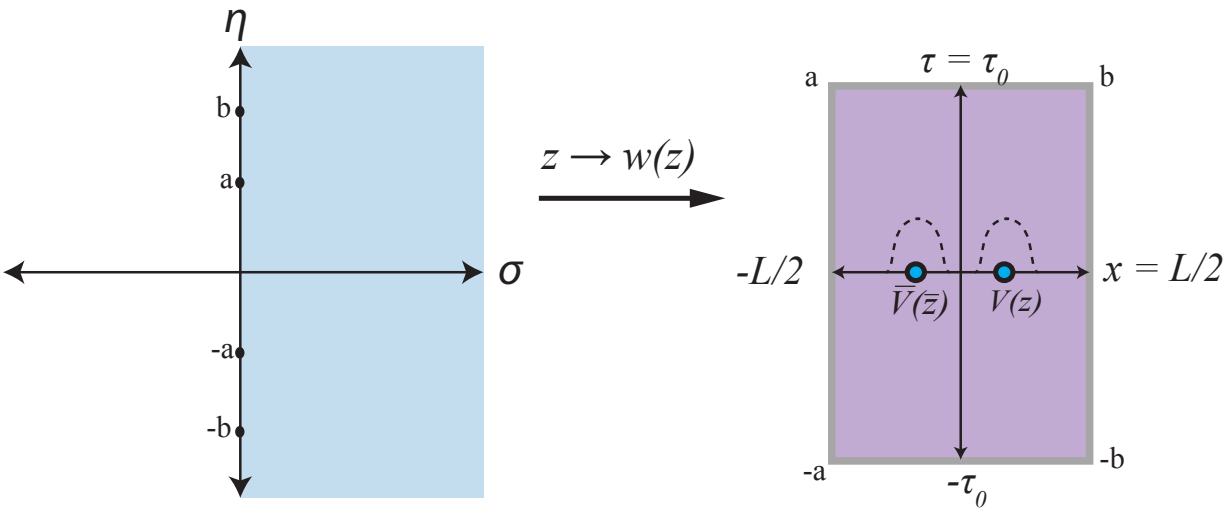

Figure 3.1: The Schwarz-Christoffel tranformation taking the right-half plane to the rectangle with chiral and antichiral vertex operators inserted on the vertical midline, $\tau = 0$

where τ_0 is the extrapolation length of the previous section. As in the case of the map (2.3.4) from the UHP, the mapping (3.1.1) is doubly-periodic[2] (i.e. with one period equal to $2L$) in the (real) argument[3] for $\tau_0 > 0$, though the period may change with operator insertions. This makes this choice of boundary state geometry particularly well-suited for modeling harmonically-confined systems.

In what follows we consider perturbations of this state obtained by vertex operator insertions in order to draw an analogy with the quench of the "Quantum Newton's Cradle" system [43] and examine the behavior of the corresponding observable. It is important to note that unlike in the previous chapter, the intent here is not to determine whether or not this system thermalizes; rather, it is to draw a parallel between the CFT behavior and that of a realistic system away from this critical point and present a compelling case for the physical significance of CFT boundary states in the study of quench dynamics away from the critical point.

[2]As shown in [56] and in Chapter 2, the ground-state stress tensor expectation value has periodicity L as the Jacobi elliptic functions only appear squared.

[3]As a result of the continuation to Lorentzian time all arguments considered here are real.

3.2 Vertex operator insertions and the split momentum quench

We note that while the analysis here is carried out for $c = 1$ CFT (free boson), the formalism described below carries over with minor modifications to $c < 1$ minimal models through the addition of screening charges to all correlation functions. We consider the free boson action

$$S = \frac{g}{2} \int d^2x \left(\nabla\phi(\vec{x})\right)^2, \tag{3.2.1}$$

where ϕ is a bosonic field, which we take to be compactified on a circle of radius R, $\phi \sim \phi + 2\pi R$, which we henceforth set to $R = 1$. Highest-weight states are given by the action of vertex operators on the vacuum state, $|n, m\rangle = \lim_{z,\bar{z}\to 0} V_{nm}(z, \bar{z})\,|0\rangle$, where $V_{nm}(z, \bar{z}) = V_{nm}(z) \otimes V_{\bar{n}\bar{m}}(\bar{z})$, and the chiral and antichiral vertex operators are given respectively as $V_{nm}(z) =: e^{i\alpha_{nm}\phi(z)} :$ and $V_{\bar{n}\bar{m}}(\bar{z}) =: e^{i\bar{\alpha}_{nm}\bar{\phi}(\bar{z})} :$, where m is the winding number and n is the wave number [77].

Their holomorphic and antiholomorphic conformal dimensions are given by

$$h_{nm} = \frac{\alpha_{nm}^2}{8\pi g} = \frac{1}{8\pi g}\left(n + \frac{m}{2}\right)^2,$$
$$\bar{h}_{nm} = \frac{\bar{\alpha}_{nm}^2}{8\pi g} = \frac{1}{8\pi g}\left(n - \frac{m}{2}\right)^2.$$

A Luttinger liquid CFT, for instance, is obtained by setting the normalization $g = K$ in (3.2.1), where K is the Luttinger parameter. The bosonic field ϕ now represents propagating density fluctuations and is related to the dual variable θ under the T-duality transformation $\phi \leftrightarrow \theta$ and $K \leftrightarrow 1/K$, $n \leftrightarrow m$. For the comparison with the experimental data in the following section we will set $g = K$ in subsequent calculations.

To implement the split-momentum quench we insert in the rectangle boundary state geometry a pair of chiral $V_{nm}(z)$ and antichiral $V_{\bar{n}\bar{m}}(\bar{z})$ vertex operators of the compactified free boson (Fig. 3.1). The opposite-chirality vertex operators act to excite the ground state in analogy to the experimental setup of two excited oppositely-moving clouds of bosons. In the CFT analogy, each such cloud is represented as a peak given by the location of the vertex

operator; in reality the clouds have a certain spread, and we later discuss how this spread can be accounted for in the CFT analysis. The Dirichlet conditions in conjunction with the inherent periodicity of the conformal mapping are implemented to mimick the harmonic trapping potential of the experimental setup.

The Dirichlet condition selects the type of boundary states allowed [99–101], which are given by [102, 103]

$$||D\rangle\rangle = (4\pi K)^{-\frac{1}{4}} \sum_{n\in\mathbb{Z}} e^{i\frac{n\phi_0}{\sqrt{4\pi K}}} |(n,0)\rangle\rangle_D \tag{3.2.2}$$

where ϕ_0 is canonically conjugate to the zero mode of the free boson and takes values in a circle of radius $R = 1$. The normalization $(4\pi K)^{-\frac{1}{4}}$ [104] is the g-factor (boundary entropy) [105] for the Dirichlet boundary condition for the action (3.2.1) with $g = K$. Unlike in the boundary-less case, expectation values of primary operators do not in general vanish in a BCFT (see, e.g. (2.3.5)); in the case of the compactified boson the expectation value can be obtained from the boundary states above as

$$\langle V_{nm}(z,\bar{z})\rangle_D = \frac{1}{\sqrt{K_0}} e^{i\frac{n\phi_0}{K_0}} |z-\bar{z}|^{-\frac{n^2}{K_0^2}} \tag{3.2.3}$$

where $K_0 = \sqrt{4\pi K}$.

The energy density expectation value $\langle\psi_0|T_{tt}(t,x)|\psi_0\rangle$ at time t for the initial state of the split-momentum quench is given, upon analytic continuation $t \to i\tau$, by

$$\frac{1}{2\pi}\left\langle\left\langle D_{\text{rec}}\right|\left|\left(T(w)+\bar{T}(\bar{w})\right)V_{nm}(w')\,V_{\bar{n}\bar{m}}(\bar{w}')\right|\right|D_{\text{rec}}\right\rangle\right\rangle \tag{3.2.4}$$

where $||D_{\text{rec}}\rangle\rangle$ is the boundary state state (3.2.2) following the conformal transformation to the rectangle, and we have used the decomposition of the energy density as the sum of holomorphic and antiholomorphic components. Coordinates on the rectangle will be denoted by $w = x + i\tau$ and on the half-plane by $z = \sigma + i\eta$. Recall that it is the Euclidean time coordinate of the stress tensor, $T_{\tau\tau}$, rather than the time coordinates of the vertex operators, that is analytically continued to Lorentzian time. The coordinates $w' = x' + i\tau'$, where $\tau' = 0$,

denote the location of the vertex operator insertion on the rectangle. The equivalence of (3.2.4) with the time-evolved expectation value of the energy density from the given initial state can be understood by noting that the right-hand side can be formally expressed as a Euclidean path integral with an operator insertion.

The expectation value (3.2.4) can be computed by conformally transforming both the vertex operators and the stress tensor to the half-plane. The vertex operators transform under the conformal transformation as primary fields, $V_{nm}(w') = \left(\frac{dw'}{dz'}\right)^{-h_{nm}} V_{nm}(z')$ and $V_{nm}(\bar{w}') = \left(\frac{d\bar{w}'}{d\bar{z}'}\right)^{-\bar{h}_{nm}} V_{nm}(\bar{z}')$, whereas the stress tensor acquires the anomalous Casimir term,

$$T(w) = \left(\frac{dw}{dz}\right)^{-2} T(z) + \frac{c}{12}\{z; w\},$$

where $\{z; w\}$ is the Schwarzian derivative as before. Note that the finite value of k, i.e. the presence of spatial boundaries, implies that the Casimir term proportional to the Schwarzian derivative that is produced by the Jacobi elliptic transformation (3.1.1) is non-constant, and it has a significant qualitative effect on the energy distribution. Employing the Ward identity on the upper-half plane [106]

$$\langle T(z)V_{nm}(z')V_{\bar{n}\bar{m}}(\bar{z}')\rangle \sim \left(\frac{\partial_{z'}}{z-z'} + \frac{h_{nm}}{(z-z')^2} + \frac{\partial_{\bar{z}'}}{z-\bar{z}'} + \frac{\bar{h}_{nm}}{(z-\bar{z}')^2}\right)\langle V_{nm}(z')V_{\bar{n}\bar{m}}(\bar{z}')\rangle$$

we arrive at the expression for (3.2.4)

$$\begin{aligned}\langle T_{\tau\tau}(w,\bar{w})\rangle = &\frac{1}{2\pi\sqrt{K_0}}\left(\frac{dw'}{dz'}\frac{d\bar{w}'}{d\bar{z}'}\right)^{-\frac{n^2}{2K_0^2}} e^{i\frac{n\phi_0}{K_0}}\,|z'-\bar{z}'|^{-\frac{n^2}{K_0^2}} \\ &\times\left\{\frac{n^2}{2K_0^2}\left(\frac{dw}{dz}\right)^{-2}\left[\frac{2}{|z'-\bar{z}'|}\left(\frac{-1}{z-z'}+\frac{1}{z-\bar{z}'}\right)+\frac{1}{(z-z')^2}+\frac{1}{(z-\bar{z}')^2}\right]\right. \\ &\left.+\frac{1}{12}\{z(w),w\}+a.h.\right\}\end{aligned} \tag{3.2.5}$$

where $a.h.$ refers to the antiholomorphic part of the expression, i.e. $z \to \bar{z}$, $w \to \bar{w}$, and as a result of the Dirichlet boundary condition we have set $h = h_{nm} = \bar{h}_{nm} = \frac{n^2}{2K_0^2}$, where as before $K_0^2 = 4\pi K$, and made use of (3.2.3) in computing the chiral-antichiral vertex

operator correlator. We stress that the coordinates z in (3.2.5) must be read as functions of the rectangle coordinates w, related via (3.1.1).

Since the transformation (3.1.1) is from the right-half plane, the antiholomorphic coordinates $\bar{z}$ are rotated from the usual upper-half plane ones, i.e. $\bar{z} = -z^*$. Finally, the Lorentzian energy expectation value $\langle T_{tt}(t,x)\rangle$ is obtained via a Wick rotation $w = x + i\tau \to x + t$ and $\bar{w} = -x + i\tau \to -x + t$.

We note that while there appear to be four divergences in (3.2.5) for all times $t > 0$, in fact two of these divergences fall outside of the rectangle boundaries at any given time, so that there are effectively only two remaining divergences. These divergences oscillate within the confines of the system, coinciding twice within each period of the full energy distribution $\langle T_{tt}(t,x)\rangle$, which is $2L$ as a result of (3.1.1). These divergences are a feature of an analysis that – despite the conformal transformation to a finite geometry – has been carried out in the thermodynamic limit. They are a consequence of the divergence of the correlation length in the thermodynamic limit: since the system that we consider here is finite of length L, the divergences are rounded off owing to the effects of finite size scaling [107] (see Appendix A for regulation scheme).

3.3 Results and comparison to experimental observations

The physical picture that emerges from (3.2.5) is that of the non-constant Casimir term, $\frac{c}{12}\{z(w), w\} + a.h.$, owing to the special type of confinement imposed, competing in strength with the two oscilating bumps (regulated divergences) of the terms involving the momentum excitations given by the vertex operator insertions. The strength of these bumps is given by the vertex operators' conformal dimension $h = \frac{n^2}{2K_0^2}$, so that the relative strength of these momentum packets to the Casimir term increases with lower values of the Luttinger parameter K. Since decreasing values of K correspond to increasing values of the Lieb-Liniger parameter γ [108], their strength increases with γ.

The elliptic Jacobi transformation with Dirichlet boundary conditions thus mimicks the

behavior observed in the "Quantum Newton's Cradle"' experiment [43], where the two momentum packets repeatedly oscillate within the harmonic trap with a periodicity such that the two packets coincide twice per period. As a result of the harmonic symmetry of the setup, in the case of the non-interacting system assumed in the CFT analysis a direct comparison is possible between position-space and momentum-space distributions: at any time t_p the momentum-space distribution is seen to be equivalent (up to an overall scale factor) to the position-space distribution at $t_x = t_p + L/2$. In the CFT analysis we have assumed that the two packets are highly localized; a realistic spread in the momentum may be accounted for by shifting the spatial coordinate away from the endpoints of the interval and closer to the middle.

Fig. 3.2 shows the regulated $\langle T_{tt} \rangle$ plots for two such shifts corresponding to a 30% spread and a 50% spread respectively at t_x intervals corresponding to integer-period t_p intervals, and at increasing values of the Luttinger parameter. We thus see the characteristic behavior of the experimental momentum-space distributions of [43], shown for comparison for decreasing initial (input) Lieb-Liniger interaction strengths in Fig. 3.3. The red curves in the experimental plots are expanded momentum distributions at single periodic times and are the observable most closely expected to correspond to the derived distributions.

3.4 Discussion

The intriguing qualitative agreement between the experimental distributions of [43] and the corresponding distributions for the analogous CFT system is not expected for a general system following a quantum quench that injects high energy into the system. It may be that the experimental parameters are such that the $c = 1$ CFT is still an approximate description of the system at the energies used in the experimental setup. However, the momenta injected during the quench are in principle above those that yield a post-quench Luttinger liquid. The findings of our analysis therefore call into question whether special features of the experimental system — possibly relating to the integrability of the system —

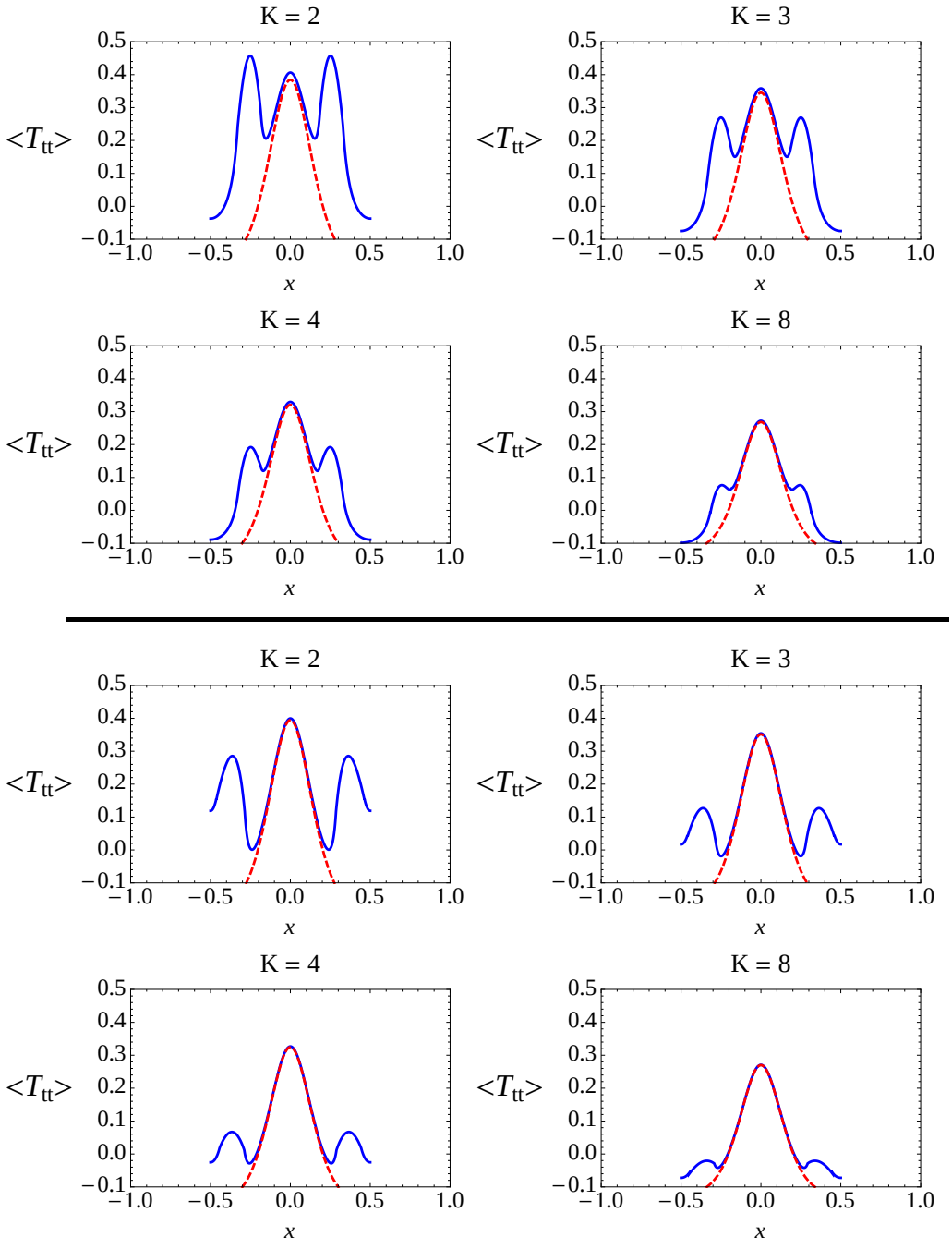

Figure 3.2: Derived regulated (see Appendix A) plots for $\langle T_{tt} \rangle$ as a function of position x from the analysis presented here for increasing values of Luttinger parameter K at $t_x = \frac{L}{2}$ and subsequent periodic intervals ($2Lm$). Up to an overall scale factor they correspond to momentum-space distributions at $t_p = 0$ and subsequent periodic intervals. Blue: full fitted distribution; dashed red: Casimir energy contribution. *Top two rows:* separation of vertex operators is $\Delta x = 0.5$; *bottom two rows:* $\Delta x = 0.3$. Parameters used were $L = 1$ and extrapolation length $\tau_0 \approx 0.278$, i.e. $k = 0.9999$. The charge of the vertex operators was set to $n = 1$. In the plots we have set $\phi_0 = 0$ in (3.2.5).

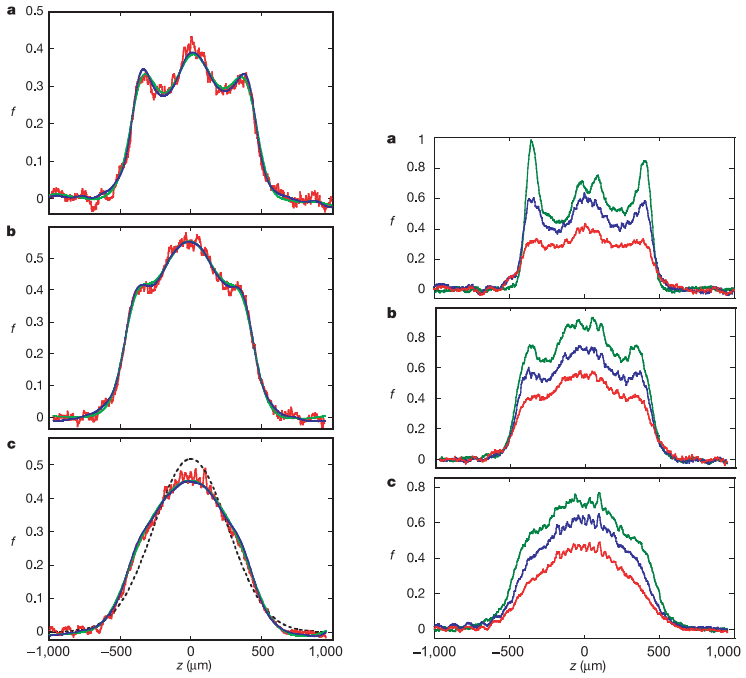

Figure 3.3: *Left:* Experimental projections [43] of the evolution of dephased momentum distributions without thermalization (based on observations after 15 oscillation periods) versus actual expanded momentum distributions for different dephased peaks coupling strengths γ_d after an integer number of periods. From top to bottom: $\gamma_d = 18$, $\gamma_d = 3.2$, $\gamma_d = 1.4$. The dashed line represents a gaussian distribution with the same number of atoms and r.m.s. width as the actual distribution. *Right:* Momentum distributions for different coupling strengths obtained by transversely integrating absorption images. Top to bottom: $\gamma = 4$, $\gamma = 1$, $\gamma = 0.62$. Reprinted by permission from Macmillan Publishers Ltd, *Nature* **440** 900903, ©2006.

lead to a post-quench relaxation towards a conformal fixed point.

It would be instructive to investigate whether a more quantitative analysis could reveal deviations from the CFT description. This can be done by placing the CFT parameters in correspondence with the analogous experimental ones, such as putting the Luttinger parameter K in numerical correspondence with the Lieb-Liniger interaction strengths [108] used in the experiment. The rectangle width, L, is representative of the horizontal momentum scale - but a proper fitting of the experimental plots necessitates knowledge of the original unscaled height of the experimental plots, to be compared with $\langle T_{tt} \rangle$ after rescaling by the appropriate constant to momentum space values. The extrapolation length τ_0 is system-

dependent, and the ability to fit this parameter could in and of itself provide interesting insight into the physics that it models. The spread of momentum in the initial peaks must also be taken into account for a proper fitting, as demonstrated in Fig. 3.3.

It is important to note that the observations of revivals in the analysis here do not in and of themselves suffice to determine whether or not the system thermalizes, as was discussed in the previous chapter. Rather, the goal of the analysis here has been twofold: (1) to motivate the physical significance of quench setups that are given by geometric forms of perturbed CFT boundary states, and (2) to demonstrate a provocative connection between the behavior of an integrable system and its conformally-invariant analog. Such a connection can be further investigated by exploring the behavior of the CFT system analyzed here as it is perturbatively deformed away from the critical point via deformations that have been shown to retain the integrability of the deformed theory (see [91, 109]).

CHAPTER 4

Electric Fields and Quantum Wormholes

The past decade has seen accumulating evidence of a deep connection between classical spacetime geometry and the entanglement of quantum fields. As described in Chapter 1, in the AdS/CFT context there appears to be a precise *holographic* sense in which a classical geometry is "emergent" from quantum entanglement in a dual field theory (see e.g. [2–6, 11, 27, 28, 110, 111]).

Recently, Maldacena and Susskind have made a stronger statement: that the link between entanglement and geometry exists even without any holographic changes of duality frame [12]. They propose that *any* entangled perturbative quantum matter in the bulk of a dynamical theory of gravity, such as an entangled Einstein-Podolsky-Rosen (EPR) [112] pair of electrons, is connected by a "quantum wormhole," or some sort of Planckian, highly fluctuating, version of the classical Einstein-Rosen (ER) [113] bridge that connects the two sides of an eternal black hole. Notably, while it clearly resonates well with holographic ideas [114–129], this "ER = EPR" proposal is more general in that it makes no reference to gauge-gravity duality. The entangled quantum fields here exist already in a theory of dynamical gravity rather than in a holographically dual field theory.

It is not at all obvious that quantum wormholes so defined – i.e. just ordinary entangled perturbative matter – exhibit properties similar to those of classical wormholes. For example, if we have dynamical electromagnetism, then the existence of a smooth geometry in the throat of an Einstein-Rosen bridge means that there exist states with a continuously tunable[1]

[1]Note that here and throughout the rest of the chaper, the word "tunable" means only that there exists a family of states where the expectation value of the flux is continuously tunable. The flux cannot actually be tuned by any local observer, as the two sides of the wormhole are causally disconnected. There does exist a quantum tunneling process in which such flux-threaded black holes can be created from the vacuum in the

electric flux threading the wormhole, as shown in Figure 4.1. Wheeler has described such states as "charge without charge" [131].

On the other hand, the two ends of a quantum wormhole may be entangled but are not connected by a smooth geometry. One might naively expect that Gauss's law would then preclude the existence of states with a continuously tunable electric flux through the wormhole. The main point of this paper is to demonstrate that this intuition is misleading: we will show that a quantum wormhole, made up of only entangled (and charged) perturbative matter, also permits electric fields to thread it in a manner that to distant observers with access to information about both sides appears qualitatively the same as that for a classical ER bridge. As we will show, for this equivalence to hold, it is crucial that there exist sufficiently light perturbative matter that is charged under the $U(1)$ gauge field. It is interesting to note that similar constraints on the charge spectrum in theories of quantum gravity have been conjectured on different grounds [132].

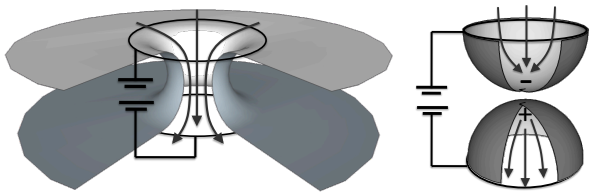

Figure 4.1: *L*eft: a classical Einstein-Rosen bridge with an applied potential difference has a tunable electric field threading it. *R*ight: A "quantum wormhole", – i.e. charged perturbative matter prepared in an entangled state, with no explicit geometric connection between the two sides also has a qualitatively similar electric field threading it.

To quantify this, for any state $|\psi\rangle$ of either system we define a dimensionless quantity called the *w*ormhole electric susceptibility χ_Δ,

$$\chi_\Delta \equiv \langle\psi|\Phi_\Delta^2|\psi\rangle \tag{4.0.1}$$

with Φ_Δ the electric flux through the wormhole. This quantity clearly measures fluctuations of the flux, and we show below that through linear response it also determines the flux

presence of a strong electric field [130].

obtained when a potential difference is applied across the wormhole. This susceptibility is a particular measure of electric field correlations across the two sides that can be interpreted as measuring how easily an electric field can penetrate the wormhole. We note that it is a global quantity that requires knowledge of the entire state: as we show explicitly below, measuring the wormhole susceptibility requires access to information about the flux on both sides, and therefore no information is transmitted across the wormhole with this electric field.

In Section 4.1 we compute this susceptibility for a classical ER bridge and in Section 4.2 for EPR entangled matter and compare the results. In Section 4.3 we discuss how one might pass a Wilson line through a quantum wormhole. In Section 4.4 we discuss what conditions the quantum wormhole should satisfy for its throat to satisfy Gauss's law for electric fields and conclude with some implications and generalizations of these findings.

Our results do not depend on a holographic description and rely purely on considerations from field theory and semiclassical relativity.

4.1 Classical Einstein-Rosen bridge

We first seek a precise understanding of what it means to have a continuously tunable electric flux through a classical wormhole. We begin with the action

$$S = \int d^4x\sqrt{-g}\left(\frac{1}{16\pi G_N}R - \frac{1}{4g_F^2}F^2\right) \ . \tag{4.1.1}$$

where g_F denotes the $U(1)$ gauge coupling. On general grounds we expect that in any theory of quantum gravity all low-energy gauge symmetries, including the $U(1)$ above, should be *c*ompact [132, 133]. This implies that the specification of the theory requires another parameter: the minimum quantum of electric charge, q. Throughout this paper we will actually work on a fixed background, not allowing matter to backreact: thus we are working

in the limit[2] $G_N \to 0$.

4.1.1 Wormhole electric susceptibility

This action admits the eternal Schwarzschild black hole as a classical solution. It has two horizons which we henceforth distinguish by calling one of them "left" and the other "right". They are connected in the interior by an Einstein-Rosen bridge [113]. On each side the metric is

$$ds^2 = -\left(1 - \frac{r_h}{r}\right) dt^2 + \frac{dr^2}{\left(1 - \frac{r_h}{r}\right)} + r^2 d\Omega_2 \qquad r > r_h, \tag{4.1.2}$$

and at $t = 0$ the two sides join at the bifurcation sphere at $r = r_h$. The inverse temperature of the black hole is given by $\beta = 4\pi r_h$.

We now surround each horizon with a spherical shell of (coordinate) radius $a > r_h$. Consider the net electric field flux through each of these spheres:

$$\Phi_{L,R} \equiv \frac{1}{g_F^2} \int_{S^2} d\vec{A} \cdot \vec{E}_{L,R}, \tag{4.1.3}$$

where the orientation for the electric field on the left and right sides is shown in Figure 4.2.

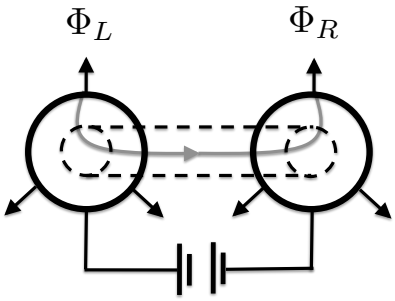

Figure 4.2: Electric fluxes for an Einstein-Rosen bridge. Black arrows indicate sign convention chosen for fluxes. Electric field lines thread the wormhole, changing the value of $\Phi_\Delta \equiv (\Phi_R - \Phi_L)/2$, when a potential difference is applied across the two sides.

There is an important distinction between the *total* flux and the *difference* in fluxes,

[2] If we studied finite G_N, allowing for the back-reaction of the electric field on the geometry, then at the non-linear level in μ we would find instead the two-sided Reissner-Nordstrom black hole. For the purposes of linear response about $\mu = 0$ this reduces to the Schwarzschild solution studied here.

defined, respectively, as

$$\Phi_\Sigma \equiv \Phi_R + \Phi_L \qquad \Phi_\Delta \equiv \frac{1}{2}(\Phi_R - \Phi_L) \ . \tag{4.1.4}$$

Via Gauss's law, the total flux Φ_Σ simply counts the total number of charged particles inside the Einstein-Rosen bridge. It is "difficult" to change, in that changing it actually requires the addition of charged matter to the action (4.1.1). Furthermore it will always be quantized in units of the fundamental electric charge q.

On the other hand, Φ_Δ measures instead the electric field *through* the wormhole. It appears that it can be continuously tuned.

We present a short semiclassical computation to demonstrate what we mean by this. We set up a potential difference $V = 2\mu$ between the left and right spheres by imposing the boundary conditions $A_t(r_R = a) = \mu$, $A_t(r_L = a) = -\mu$. This is a capacitor with the two plates connected by an Einstein-Rosen bridge. The resulting electric field in this configuration can be computed by solving Maxwell's equations, which are very simple in terms of the conserved flux

$$\Phi = \frac{1}{g_F^2}\int d^2\Omega_2 \ r^2 F_{rt} \qquad \partial_r \Phi = 0 \ . \tag{4.1.5}$$

As there is no charged matter all the different fluxes are equivalent: $\Phi_R = -\Phi_L = \Phi_\Delta$. By symmetry we have $A_t(r_h) = 0$, and so we have

$$\mu = A_t(r_R = a) = \int_{r_h}^{a} dr F_{rt} = \Phi \frac{g_F^2}{4\pi}\left(\frac{1}{a} - \frac{1}{r_h}\right) \ . \tag{4.1.6}$$

We now take $a \to \infty$ for simplicity to find:

$$\Phi_\Delta = \left(\frac{4\pi r_h}{g_F^2}\right)\mu \tag{4.1.7}$$

As we tune the parameter μ, Φ_Δ changes continuously as we pump more electric flux through

the wormhole. There is thus a clear qualitative difference between Φ_Δ and the quantized total flux Φ_Σ. In this system the difference arose entirely from the fact that there is a geometric connection between the two sides.

We now seek a quantitative measure of the strength of this connection. The prefactor relating the flux to small fluctuations of μ away from zero in (4.1.7) is a good candidate. To understand this better, we turn now to the full quantum theory of $U(1)$ electromagnetism on the black hole background. The prefactor is actually measuring the fluctuations of the flux Φ_Δ around the $\mu = 0$ ground state of the system and is equivalent to the wormhole electric susceptibility defined in (4.0.1):

$$\chi_\Delta \equiv \langle\psi|\Phi_\Delta^2|\psi\rangle \ . \tag{4.1.8}$$

To see this, recall that we are studying the Hartle-Hawking state for the Maxwell field. When decomposed into two halves this state takes the thermofield double form [110, 134]:

$$|\psi\rangle \equiv \frac{1}{\sqrt{Z}} \sum_n |n^*\rangle_L |n\rangle_R \exp\left(-\frac{\beta}{2} E_n\right) \ . \tag{4.1.9}$$

Here L and R denote the division of the Cauchy slice at $t = 0$ into the left and right sides of the bridge, n labels the exact energy eigenstates of the Maxwell field, E_n denotes the energy with respect to Schwarzschild time t, and $|n^*\rangle$ is the CPT conjugate of $|n\rangle$ [3].

The two-sided black hole has a non-trivial bifurcation sphere S^2. The electric flux through this S^2 is a quantum degree of freedom that can fluctuate. In the decomposition above we have two separate operators $\Phi_{L,R}$, both of which are conserved charges with discrete spectra, quantized in units of q: $\Phi = q\mathbb{Z}$. Each energy eigenstate can be picked to have a definite flux Φ_n: $|n, \Phi_n\rangle$. Importantly, CPT preserves the energy but flips the sign of the flux. Schematically, we have:

$$\text{CPT}|n, \Phi_n\rangle = |n, -\Phi_n\rangle \ . \tag{4.1.10}$$

This means that each L state in the sum (4.1.9) is paired with an R state of opposite flux,

[3] The pairing of a state $|n\rangle$ with its CPT conjugate $|n^\star\rangle$ can be understood as following from path-integral constructions of the thermofield state by evolution in Euclidean time.

and so the state is annihilated by $\Phi_L + \Phi_R$:

$$(\Phi_L + \Phi_R)|\psi\rangle = 0 \tag{4.1.11}$$

This relation is Gauss's law: every field line entering the left must emerge from the right.

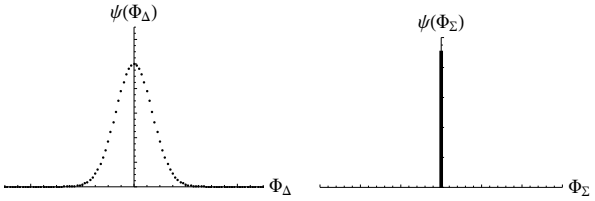

Figure 4.3: Wavefunction of the Maxwell state as a function of discrete fluxes Φ_Δ and Φ_Σ. The spread in Φ_Δ is measured by the wormhole susceptibility χ_Δ. The wavefunction has no spread in Φ_Σ.

On the other hand, Φ_Δ does *n*ot have a definite value on this state: as Φ_Δ does not annihilate $|\psi\rangle$, the wavefunction has a spread centered about zero, as shown in Figure 4.3. The spread of this wavefunction is measured by the wormhole susceptibility (4.1.8). The intuitive difference between Φ_Σ and Φ_Δ discussed above can be traced back to the fact that the wavefunction is localized in the former case and extended in the latter.

The location of this maximum is not quantized and can be continuously tuned. For example, let us deform (4.1.9) with a chemical potential μ:

$$|\psi(\mu)\rangle \equiv \frac{1}{\sqrt{Z}} \sum_n |n^*\rangle_L |n\rangle_R \exp\left(-\frac{\beta}{2}(E_n - \mu\Phi_n)\right) . \tag{4.1.12}$$

Similarly deformed thermofield states and the existence of flux through the Einstein-Rosen bridge have been recently studied in [135–137]. Expanding this expression to linear order in μ we conclude that

$$\langle\psi(\mu)|\Phi_\Delta|\psi(\mu)\rangle = \beta\mu\chi_\Delta + \cdots \tag{4.1.13}$$

with χ_Δ the wormhole susceptibility (4.1.8) evaluated on the undeformed state (4.1.9)[4]. This

[4]The discussion in the bulk of the text assumes that we work only to linear order in μ. If we relax this

expectation value is the precise statement of what was computed semiclassically in (4.1.7)[5]: comparing these two relations we see that the wormhole susceptibility for the black hole is

$$\chi_\Delta^{\rm ER} = \frac{1}{g_F^2} \ . \tag{4.1.15}$$

4.1.2 Quantization of flux sector on black hole background

It is instructive to provide a more explicit derivation of (4.1.15) by computing the full wavefunction as a function of Φ_Δ. This requires the determination of the energy levels E_n in (4.1.12). We study the free Maxwell theory on a fixed background, neglecting gravitational backreaction. As we are interested in the *total* flux, we need only determine an effective Hamiltonian describing the quantum mechanics of the flux sector. We ignore fluctuations in $A_{\theta,\phi}$ and any angular dependence of the fields, integrating over the S^2 in (4.1.1) to obtain the reduced action:

$$S = -\frac{2\pi}{g_F^2}\int dr dt \sqrt{-g} g^{rr} g^{tt} (F_{rt})^2 \ . \tag{4.1.16}$$

To compute the E_n we pass to a Hamiltonian formalism with respect to Schwarzschild time t. We first consider the Hilbert space of the right side of the thermofield double state (4.1.9). The canonical momentum conjugate to A_r is the electric flux:

$$\Phi \equiv \frac{\delta \mathcal{L}}{\delta \partial_t A_r} = \frac{4\pi}{g_F^2}\sqrt{-g} F^{rt} \ . \tag{4.1.17}$$

assumption then (4.1.13) is replaced by

$$\frac{d}{d\mu}\langle \Phi_\Delta \rangle_\mu = \beta \left(\langle \Phi_\Delta^2 \rangle - \langle \Phi_\Delta \rangle^2 \right)_\mu , \tag{4.1.14}$$

where the right-hand side is now the appropriate generalization of the wormhole electric susceptibility to nonzero μ, reducing to (4.1.8) in the limit that $\mu \to 0$.

[5]More precisely: the classical relation (4.1.7) amounts to a saddle-point evaluation of a particular functional integral which evaluates expectation values of (4.1.9).

A_t does not have a conjugate momentum. The Hamiltonian is constructed in the usual way as $H \equiv \Phi \partial_t A_r - \mathcal{L}$ and is

$$H = \int_{r_h}^{\infty} dr \left(-\frac{g_F^2}{8\pi\sqrt{-g} g^{rr} g^{tt}} \Phi^2 - (\partial_r \Phi) A_t \right) + \Phi(A_t(r_h) - A_t(\infty)) \tag{4.1.18}$$

where we have integrated by parts. The equation of motion for A_t is Gauss's law, setting the flux to a constant: $\partial_r \Phi = 0$.

There are two boundary terms of different character. The value of $A_t(\infty) \equiv \mu$ at infinity is set by boundary conditions. If μ is nonzero, then the Hamiltonian is deformed to have a chemical potential for the flux as in (4.1.12). Recall, however, that the susceptibility is defined in the undeformed state, as in (4.0.1). For the remainder of this section we therefore set μ to zero. On the other hand, $A_t(r_h)$ is a dynamical degree of freedom. We should thus combine this Hamiltonian with the corresponding one for the left side of the thermofield state; demanding that the variation of the horizon boundary term with respect to $A_t(r_h)$ vanishes then requires that $\Phi_L = -\Phi_R$, as expected from (4.1.11).

As the flux is constant we may now perform the integral over r to obtain the very simple Hamiltonian

$$H = G\Phi^2 \qquad G \equiv -\int_{r_h}^{\infty} dr \frac{g_F^2}{8\pi\sqrt{-g} g^{rr} g^{tt}} = \frac{g_F^2}{8\pi r_h} \tag{4.1.19}$$

This Hamiltonian describes the energy cost of fluctuations of the electric field through the horizon of the black hole.

The flux operator in the reduced Hilbert space[6] of the flux sector acts as

$$\Phi|m\rangle = qm|m\rangle \qquad m \in \mathbb{Z} \tag{4.1.20}$$

where $m \in \mathbb{Z}$ denotes the number of units of flux carried by each state $|m\rangle$. The Hamiltonian (4.1.19) is diagonal in this flux basis, with the energy of a state with m units of flux given

[6]Where, as above, we neglect fluctuations along the angular directions.

by

$$E_m = \frac{g_F^2}{8\pi r_h}(qm)^2 \qquad m \in \mathbb{Z} \tag{4.1.21}$$

Though we do not actually need it, for completeness we note that the operator that changes the value of the flux through the S^2 is a spacelike Wilson line that pierces it carrying charge q:

$$W = \exp\left(iq \int dr A_r\right) \ . \tag{4.1.22}$$

Indeed from the fundamental commutation relation $[A_r(r), \Phi(r')] = i\delta(r - r')$ we find the commutator

$$[W, \Phi] = -qW, \tag{4.1.23}$$

meaning that a Wilson line that pierces the S^2 once increases the flux by q. In our case any Wilson line that pierces the left sphere must continue to pierce the right: thus if it increases the left flux it will decrease the right flux, and we are restricted to the gauge-invariant subspace that is annihilated by $\Phi_L + \Phi_R$.

Thus we see that the thermofield state (4.1.9) in the flux sector takes the simple form:

$$|\psi\rangle = \frac{1}{\sqrt{Z}} \sum_{m\in\mathbb{Z}} |-m\rangle|m\rangle \exp\left(-\frac{g_F^2}{4}(qm)^2\right), \tag{4.1.24}$$

where we have used $\beta = 4\pi r_h$. Since $\Phi_\Delta = \Phi_R$ on this state, the probability of finding any flux Φ_Δ through the black hole is simply

$$P(\Phi_\Delta) = \frac{1}{Z} \exp\left(-\frac{g_F^2}{2}\Phi_\Delta^2\right) \ . \tag{4.1.25}$$

This is the (square of the) wavefunction shown in Figure 4.3: even though Φ_Δ has a discrete spectrum, the wavefunction is extended in Φ_Δ. In the semiclassical limit $(g_F q) \to 0$ the discreteness of Φ_Δ can be ignored and the spread $\chi_\Delta = \langle \Phi_\Delta^2 \rangle$ is again $\chi_\Delta^{\text{ER}} = g_F^{-2}$, in agreement with the result found from the classical analysis (4.1.15). This result is exact only for the free Maxwell theory on a fixed background: if we study an interacting theory

(e.g. by including gravitational backreaction or charged matter) then the wavefunction will no longer be a pure Gaussian and (4.1.25) will receive nonlinear corrections in Φ_Δ.

The probability distribution exhibited in (4.1.25) may be surprising as it shows that an observer hovering outside an uncharged eternal black hole nevertheless finds a nonzero probability of measuring an electric flux through the horizon. However, due to (4.1.11) the flux measured by the right observer will always be precisely anti-correlated with that measured by the left observer. These observers are measuring fluctuations of the field *t*hrough the wormhole, not fluctuations of the number of charges inside. Through (4.1.13) we see that it is actually the presence of these fluctuations that makes it possible to tune the electric field through the wormhole. In the above analysis, we have computed the fluctuations in the Hartle-Hawking state; more generally, any nonsingular state of the gauge fields in the ER background will have correlated fluctuations in the flux, arising from the correlated electric fields near the horizon.

4.2 Quantum wormhole

We now consider the case of charged matter in an entangled state but with no geometrical, and hence no gravitational, connection. We will show below that when we apply a potential difference, an appropriate pattern of entanglement between the boxes is sufficient to generate a non-vanishing electric field even though the two boxes are completely noninteracting.

The configuration that we study here is that of a complex scalar field ϕ charged under a $U(1)$ symmetry (with elementary charge q), confined to two disconnected spherical boxes of radius a, as shown in Figure 4.4. The confinement to $r < a$ is implemented by imposing Dirichlet boundary conditions for the fields. These boundary conditions still allow the radial electric field to be nonzero at the boundary, so our main observable, the electric flux, is not constrained by the boundary conditions.

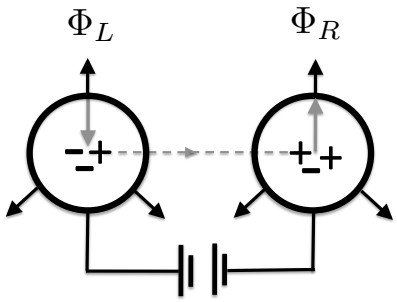

Figure 4.4: Setup for the quantum wormhole. The two boxes are geometrically disconnected but contain a scalar field in an entangled state. Correlated charge fluctuations effectively allow electric field lines to travel from one box to the other when a potential difference is applied.

The action in each box is

$$S = \int d^4x\sqrt{-g}\left(-|D\phi|^2 - m^2\phi^\dagger\phi - \frac{1}{4g_F^2}F^2\right) . \tag{4.2.1}$$

where $D_\mu\phi = \partial_\mu\phi - iqA_\mu\phi$. This is now an interacting theory where the perturbative expansion is controlled by $(g_F q)^2$.

Gauss's law relates the electric flux to the total global charge Q. Thus we have the following operator equation on physical states:

$$\Phi = \frac{1}{g_F^2}\int d^3x\,(\nabla\cdot E) = Q. \tag{4.2.2}$$

At first glance this situation is rather different from the classical black hole case. Φ_L and Φ_R simply measure the number of particles in the left and right boxes respectively. There appears to be no difference between Φ_Σ and Φ_Δ and thus no way to thread an electric field through the boxes. This intuition is true in the vacuum of the field theory, which is annihilated by both Φ_L and Φ_R. As it turns out, it is wrong in an entangled state.

Let us now perform the same experiment as for the black hole: we will set up a potential difference of 2μ between the two spheres by studying the analog of the deformed thermofield state (4.1.12). We will work at weak coupling: the only effect of the nonzero coupling is to relate the flux to the global charge as in (4.2.2). We are thus actually studying charge

fluctuations of the scalar field. These charge fluctuations source electric fields which cost energy, but this energetic penalty can be neglected at lowest order in the coupling[7].

The full state for the combined Maxwell-scalar system is formally the same as (4.1.12). We schematically label the scalar field states by their energy and global charge as $|n, Q_n\rangle$. Due to the constraint (4.2.2), the scalar field sector of the thermofield state can be written:

$$|\psi(\mu)\rangle \equiv \frac{1}{\sqrt{Z}} \sum_n |n, -Q_n\rangle_L |n, Q_n\rangle_R \exp\left(-\frac{\beta}{2}\left(E_n - \mu Q_n\right)\right) \tag{4.2.3}$$

This state corresponds to having a constant value of $A_t = \mu$ in the right sphere and $A_t = -\mu$ in the left sphere. Note that we have

$$(\Phi_L + \Phi_R)|\psi(\mu)\rangle = (Q_L + Q_R)|\psi(\mu)\rangle = 0 \ . \tag{4.2.4}$$

We now seek to compute $\langle \Phi_\Delta \rangle_\mu = \langle Q_\Delta \rangle_\mu = \langle Q_R \rangle_\mu$ where the second equality follows from (4.2.4). However to compute $Q_R(\mu)$ we can trace out the left side. Tracing out one side of the thermofield state results in a thermal density matrix for the remaining side: thus we are simply performing a standard statistical mechanical computation of the charge at finite temperature and chemical potential. Details of this computation are in Appendix B, and the result is:

$$\langle \Phi_\Delta \rangle_\mu = q^2 \sum_n \left(\frac{1}{1 - \cosh(\beta\omega_n)}\right)(\beta\mu) + \mathcal{O}(\mu^2), \tag{4.2.5}$$

where the ω_n are the single-particle energy levels. The sum can be done numerically.

We conclude that the wormhole susceptibility for this state is:

$$\chi_\Delta^{\text{EPR}} = q^2 f\left(m\beta, ma\right) \tag{4.2.6}$$

with f a calculable dimensionless function that is $O(1)$ in the couplings and is displayed for illustrative purposes in Figure 4.5. Crudely speaking it measures the number of accessible

[7] It is interesting to note that in the black hole case the key difference is that the energy cost associated to the gauge fields – which we neglect in this case – is the *l*eading effect.

charged states. If we decrease the entanglement by lowering the temperature, the susceptibility vanishes exponentially as $f \sim \exp(-\omega_0 \beta)$, with ω_0 the lowest single-particle energy level. Its precise form – beyond the fact that it is nonzero in the entangled state – is not important for our purposes.

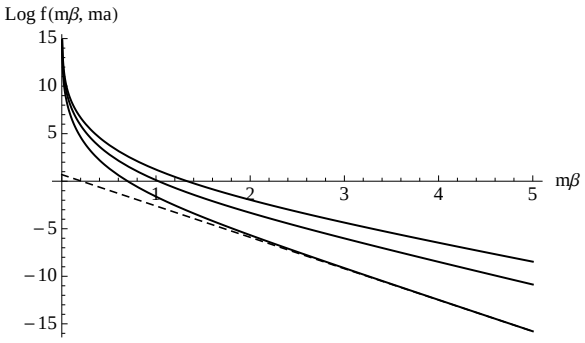

Figure 4.5: Numerical evaluation of the logarithm of the dimensionless function $f(m\beta, ma)$ appearing in wormhole susceptibility for complex scalar field. From bottom moving upwards, three curves correspond to $ma = 1, 1.5, 2$. Dashed line shows asymptotic behavior for $ma = 1$ of $\exp(-\omega_0 \beta)$.

We see then that as a result of the potential difference that we have set up between the two entangled spheres, we are able to measure flux fluctuations across the wormhole that are both continuously tunable and fully correlated with each other: this is observationally indistinct from measuring an electric field through the wormhole. This field exists not because of geometry, but rather because the electric field entering one sphere attempts to create a negative charge. Due to the entanglement this results in the creation of a positive charge in the other sphere, so that the resulting field on that side is the same electric field as the one entering the first sphere. This appears rather different from the mechanism at play for a geometric wormhole, but the key fact is that the wavefunction in the flux basis takes qualitatively the same form (i.e. that shown in Figure 4.3) for both classical and quantum wormholes, meaning that the universal response to electric fields is the same for both systems.

Quantitatively, however, there is an important difference. If the function f that measures the number of charged states is of $O(1)$, then the wormhole susceptibility for the quantum wormhole (4.2.6) is smaller than that for the classical wormhole (4.1.15) by a factor of

$(g_F q)^2$. It is *much* harder – i.e. suppressed by factors of $\hbar$ – to push an electric field through a quantum wormhole. Alternatively, we can view (4.1.15) as defining the value of the $U(1)$ gauge coupling in the wormhole region. In the quantum wormhole we have succeeded in creating a putative region through which a $U(1)$ gauge field can propagate, but its coupling there (as measured by (4.2.6)) is large, and becomes larger as the entanglement is decreased. Notwithstanding these large "quantum fluctuations", the quantum wormhole does nevertheless satisfy topological constraints such as Gauss's law.

Despite this suppression, there is no obstruction in principle to making f sufficiently large so that the susceptibilities can be made the same. Increasing the temperature or the size of the box will increase the number of charged states and thus increase f, as can be seen explicitly in Figure 4.5. Thus even the numerical value of the EPR wormhole susceptibility can be made equal or even greater than that of the ER bridge, although we will require a large number of charged particles to do it in a weakly coupled regime.

4.3 Wilson lines through the horizon

It was argued above that electric flux measurements behave qualitatively the same for a classical and for a quantum wormhole. It is interesting to consider other probes involving the gauge field. For example, the classical eternal black hole also allows a Wilson line to be threaded through it. Such Wilson lines have recently been studied in a toy model of holography in [137]. For the black hole, consider extending a Wilson line from the north pole of the left sphere at $r = a$ through the horizon to the north pole of the right sphere:

$$W_{ER} = \left\langle \exp\left(iq \int_L^R A \right) \right\rangle \approx 1 \tag{4.3.1}$$

Since we assume that the gauge field is weakly coupled throughout the geometry, to leading order we can simply set it to 0, leading to the approximate equality above.

On the other hand, in the entangled spheres case where there is no geometric connection it

is not clear how a Wilson line may extend from one box to the other. However, an analogous object with the same quantum numbers as (4.3.1) is

$$W_{EPR} = \left\langle \exp\left(iq\int_L^0 A_L\right)\phi_L(0)\phi_R^\dagger(0)\exp\left(iq\int_0^R A_R\right)\right\rangle, \tag{4.3.2}$$

where each Wilson line extends now from the skin of the sphere to the center of the sphere at $r = 0$, where it ends on a charged scalar field insertion.

While the gauge field may be set to zero as in the black hole case above, we must furthermore account for the mixed correlator of the scalar field, which is nonzero only due to entanglement. Details of the computation and a plot of the results can be found in Appendix B. The leading large β behavior is

$$W_{EPR} \sim \exp\left(-\frac{\omega_0\beta}{2}\right) . \tag{4.3.3}$$

As the temperature is decreased the expectation value of the Wilson line vanishes, consistent with the idea put forth above that the gauge field living in the wormhole is subject to strong quantum fluctuations which become stronger, washing out the Wilson line, as the entanglement is decreased.

4.4 Discussion

A classical geometry allows an electric field to be passed through it. We have demonstrated here that we can mimic this aspect of a geometric connection using entangled charged matter alone. We also introduced the wormhole susceptibility, a quantitative measure of the strength of this connection. For quantum wormholes this susceptibility is suppressed relative to that for classical wormholes by factors of the dynamical $U(1)$ gauge coupling, i.e. by powers of $\hbar$, but, as we argued in Section 4.2, there is in principle no impediment for the susceptibilities to be of the same order. The susceptibility is defined for any state, but for the thermofield state it directly measures the electric field produced when a potential difference is applied

across the wormhole.

We stress that we are not claiming that there is a smooth geometry in the quantum wormhole; however, there is a crude sense in this setup in which a geometry emerges from the presence of entanglement. We showed that by adjusting the parameters, two boxes of weakly coupled, entangled charged particles can mimic an Einstein-Rosen bridge in their response to electric potentials. The structure we have found in this highly excited state is similar to that of the vacuum of a two-site $U(1)$ lattice gauge theory, where entanglement between the sites allows the electric flux between them to fluctuate. This is enough to allow for a nonzero susceptibility and is somewhat reminiscent of ideas of dimensional deconstruction [138].

The equivalence is only at the coarse level of producing the same electric flux at the boundary of the boxes; more detailed observations inside the boxes would quickly reveal that charged matter rather than black holes are present. However, the presence of a nonzero wormhole electric susceptibility already at weak coupling, along with the fact that the two susceptibilities become similar as the coupling is increased, is compatible with the idea that as we go from weak to strong coupling entangled matter becomes an ER bridge.

It is worth noting that the quantum wormholes considered still satisfy Gauss's law (4.2.4) in that every field line entering one side must exit from the other. This is due to the correlated charge structure of the states considered:

$$|\psi\rangle \sim \sum_{Q} |-Q\rangle|Q\rangle \tag{4.4.1}$$

If we coherently increase the charge of the left sector relative to the right, then this would correspond to having a definite number of charged particles inside the wormhole.

Alternatively, we could consider a more generic state, involving instead an incoherent sum over all charges. This type of generic quantum wormhole does not satisfy any analog of Gauss's law. At first glance, this appears non-geometric, in agreement with the intuition that a generic state should not have a simple geometric interpretation [139, 140]. On the other hand, we could also simply state that we have filled the wormhole with matter that is

not in a charge eigenstate, i.e. a superconducting fluid. Thus some "non-geometric" features nevertheless have an interpretation in terms of effective field theory, and a two-sided analog of the holographic superconductor [141–143] might capture universal aspects of the gauge field response of such a state.

We note also that the susceptibility is constructed from conserved charges, and so it commutes with the Hamiltonian. Thus the time-evolved versions of the thermofield state (which have been the subject of much recent study as examples of more "generic" states [12, 54,122,129,144,145]) do not scramble charges: they all have the same wormhole susceptibility as the original thermofield state and precisely satisfy Gauss's law. We also find that the wormhole susceptibility must be conserved if two disconnected clouds of entangled matter are collapsed to form two black holes, which presumably then must have an Einstein-Rosen bridge between them. This provides a crude realization of the collapse experiment proposed in [12].

It is of obvious interest to generalize our considerations to gravitational fields. In that case the wormhole gravitational susceptibility corresponding to (4.1.15) directly measures Newton's constant in the wormhole throat. Note also that the form of the "ER = EPR" correspondence studied here requires the existence of perturbative matter charged under every low-energy gauge field: e.g. to form a quantum wormhole to have a nonzero wormhole magnetic susceptibility and thus to admit magnetic fields, we would require entangled magnetic monopoles. If the charge spectrum were not complete, one could certainly tell the difference between an ER bridge and an EPR one. Precisely such a completeness of the charge spectrum in consistent theories of quantum gravity has been conjectured on (somewhat) independent grounds [132, 133, 146].

Finally, we find it intriguing that the two computations performed here result in qualitatively similar answers, but arising from different sources and at different orders in bulk couplings. One might be tempted to speculate that in a formulation of bulk quantum gravity that is truly non-perturbative these two very different computations could be understood as accessing a more general concept that reduces in different limits to either perturbative

entanglement or classical geometry. It remains to be seen what this more general concept might be.

APPENDIX A

Divergence regulation scheme

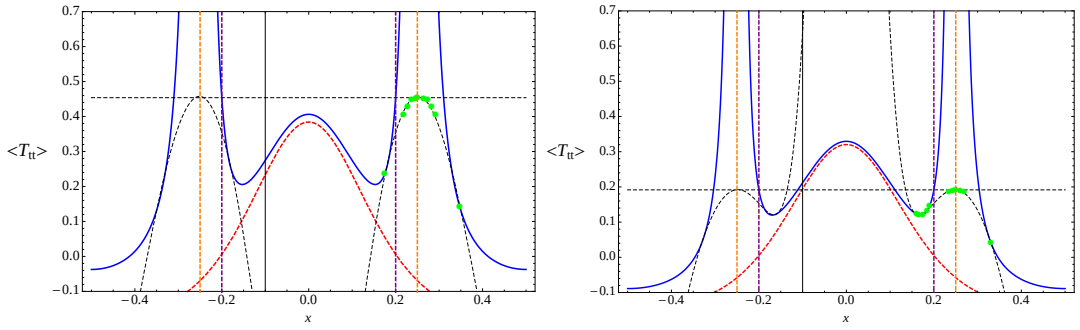

Figure A.1: Fitting scheme for divergence regulation. Left: $K = 2$, Right: $K = 4$; $\Delta x = 0.5$. Curves shown are unregulated $\langle T_{tt} \rangle$ plot (solid blue), Casimir hump (dashed red), location of singularities (dashed orange), lower bound on critical region (dashed purple), corresponding vertical cutoff (dashed black straight line), data points used for fitting (green), and numerically fitted plots (dashed black) using a normal distribution multiplied by an error function for skewness..

In the thermodynamic limit, the correlation length $\xi \sim t^{-\nu}$, where $t = \frac{|T-T_c|}{T_C}$, diverges at the critical temperature[1] $T = T_c$. The size of the critical region is then given by $t \sim \xi^{-\frac{1}{\nu}}$. In a finite-size system the correlation length is limited by the system size; the expected scaling in a trap of size L is $\xi \sim L^{\theta}$ [147–150], where θ is the trap critical exponent. Experimental systems of trapped ultracold bosons in optical lattices in one dimension are well-described by the Bose-Hubbard Hamiltonian [151] and for that model it is given by $\theta = \frac{p}{p+1/\nu}$ in the case of a power-law potential. This implies that the size of the critical region is given by $t \sim L^{-\frac{\theta}{\nu}}$. For divergences occurring at $x = x_0$ we therefore place a cutoff at the height corresponding to the left boundary of the critical region, $x = x_0 - \frac{1}{2} a L^{-\frac{\theta}{\nu}}$, where a is an arbitrary but consistent choice of constant ($a = 0.1$ in Fig. A.1), and round off the divergences at the

[1] We note that we use T_c here for illustrative purposes; in general the particular critical parameter relevant to the system should be employed to determine the critical region of the system.

corresponding height by finding a best-fit function (skewed exponential ansatz) for a set of representative points such that a smooth choice is ensured for a given choice of K. We set $\nu = 1$ and $p = 2$ (harmonic potential) for the distributions derived here.

APPENDIX B

Charged scalar field computations

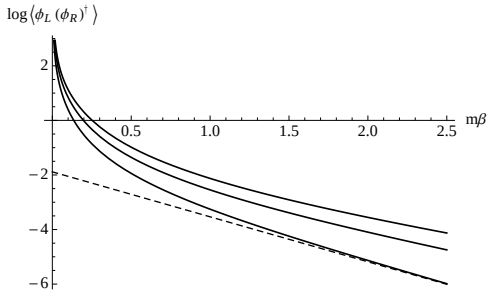

Figure B.1: Numerical evaluation of the logarithm of $\langle \phi_L(0)\phi_R^\dagger(0)\rangle$, which contributes the interesting dependence of the Wilson line (4.3.2). From bottom moving upwards, curves correspond to $ma = 1, 1.5, 2$. Dashed line corresponds to asymptotic behavior for $ma = 1$ of $\exp\left(-\frac{\omega_0}{2\beta}\right)$ with ω_0 the lowest single-particle energy level.

Here we present some details of the charged scalar field computations presented in the main text. Similar results would be obtained for essentially any system in any geometry, but for concreteness we present the precise formulas for the charged scalar field in a spherical box. The relevant part of the action is

$$S_\phi = -\int d^4x \left(|D\phi|^2 + m^2|\phi|^2\right) \tag{B.0.1}$$

The scalar field is confined to a spherical box of radius a with Dirichlet boundary conditions $\phi(r = a) = 0$. We first compute the single-particle energy levels.

Expanding the field in spherical harmonics as $\phi = \sum_{lmp} \phi_{lp}(r)e^{-i\omega t}\, Y_{lm}(\theta, \phi)$ we find the mode equation for $\phi_{lp}(r)$ to be

$$\frac{1}{r^2}\partial_r\left(r^2\partial_r\phi_{lp}(r)\right) - \frac{l(l+1)}{r^2}\phi_{lp}(r) = (m^2 - \omega^2)\phi_{lp}(r), \tag{B.0.2}$$

Here p is a radial quantum number and l is angular momentum as usual. The normalizable solutions to the radial wave equation are spherical Bessel functions of order l:

$$\phi_{lp}(r) = c_{lp} j_s(l, \lambda_{lp} r) \qquad c_{lp} = \frac{2}{\sqrt{a^3 \pi}} \left(J_{l+\frac{3}{2}}(\lambda_{lp} a) \right)^{-1} \tag{B.0.3}$$

The normalization c_{lp} has been picked such that

$$\sum_p \phi_{lp}(r) \phi_{lp}(r') = \frac{\delta(r - r')}{r^2} \tag{B.0.4}$$

In c_{lp}, $J_\nu(x)$ is an ordinary Bessel function of the first kind. Imposing the Dirichlet boundary condition fixes $\lambda_p = \frac{x_{lp}}{a}$, where x_{lp} is the p-th zero of the l-th spherical Bessel function. This determines the energy levels to be

$$\omega_{lp} = \sqrt{m^2 + \left(\frac{x_{lp}}{a} \right)^2}, \tag{B.0.5}$$

We are now interested in computing the charge susceptibility at finite temperature T and chemical potential μ. From elementary statistical mechanics we have the usual expression for the charge

$$\langle Q \rangle = q \sum_{lp} (2l + 1) \left(\frac{1}{1 - e^{\beta(\omega_{lp} + q\mu)}} - \frac{1}{1 - e^{\beta(\omega_{lp} - q\mu)}} \right), \tag{B.0.6}$$

where we have included the degeneracy factor $(2l + 1)$. Linearizing this in μ we obtain (4.2.5), where it is understood that the sum over single-particle states there includes a sum over angular momentum eigenstates: $\sum_n \to \sum_{lp} (2l + 1)$.

Next we compute the correlation function $\langle \phi_L^\dagger(0) \phi_R(0) \rangle$ across the two sides of the thermofield state (4.2.3) (with $\mu \to 0$). The fastest way to compute this is to note that the two sides of the thermofield state can be understood as being connected by Euclidean time evolution through $\frac{\beta}{2}$. Thus the mixed correlator can be calculated by computing the usual Euclidean correlator between two points separated by $\frac{\beta}{2}$ in Euclidean time (see e.g. [110]). If the single-particle energy levels are given by ω_{pl}, then the Euclidean correlator between

two general points is

$$G(\tau, r, \theta, \phi; \tau', r', \theta', \phi') = \sum_{lmp} \frac{1}{2\omega_{lp}} \frac{\cosh\left(\omega_{lp}\left(\tau - \tau' - \frac{\beta}{2}\right)\right)}{\sinh\left(\frac{\beta\omega_{lp}}{2}\right)} \times$$
$$\phi_{pl}(r)\phi_{pl}(r')Y_{lm}(\theta, \phi)Y^*_{lm}(\theta', \phi'), \tag{B.0.7}$$

where in this expression the normalization of the mode functions (B.0.4) is important.

For our application to the Wilson line in (4.3.2) we care about the specific case $\tau - \tau' = \frac{\beta}{2}$ and $r = r' = 0$. The spherical Bessel functions with nonzero angular momentum $l \neq 0$ all vanish at the origin $r = 0$. Thus the sum is only over the $l = 0$ modes. The result of performing this sum numerically is shown in Figure B.1, but it is easy to see that at small temperatures the answer will be dominated by the lowest energy level and is:

$$\langle \phi_L(0)^\dagger \phi_R(0) \rangle \sim \exp\left(-\frac{\omega_0 \beta}{2}\right) . \tag{B.0.8}$$

References

[1] J. M. Maldacena, "The Large N limit of superconformal field theories and supergravity," *Int. J. Theor. Phys.* **38** (1999) 1113–1133, arXiv:hep-th/9711200 [hep-th]. [Adv. Theor. Math. Phys.2,231(1998)].

[2] S. Ryu and T. Takayanagi, "Holographic derivation of entanglement entropy from AdS/CFT," *Phys. Rev. Lett.* **96** (2006) 181602, arXiv:hep-th/0603001 [hep-th].

[3] S. Ryu and T. Takayanagi, "Aspects of Holographic Entanglement Entropy," *JHEP* **08** (2006) 045, arXiv:hep-th/0605073 [hep-th].

[4] V. E. Hubeny, M. Rangamani, and T. Takayanagi, "A Covariant holographic entanglement entropy proposal," *JHEP* **07** (2007) 062, arXiv:0705.0016 [hep-th].

[5] M. Van Raamsdonk, "Comments on quantum gravity and entanglement," arXiv:0907.2939 [hep-th].

[6] M. Van Raamsdonk, "Building up spacetime with quantum entanglement," *Gen.Rel.Grav.* **42** (2010) 2323–2329, arXiv:1005.3035 [hep-th].

[7] B. Swingle, "Entanglement Renormalization and Holography," *Phys. Rev.* **D86** (2012) 065007, arXiv:0905.1317 [cond-mat.str-el].

[8] B. Swingle, "Constructing holographic spacetimes using entanglement renormalization," arXiv:1209.3304 [hep-th].

[9] E. Bianchi and R. C. Myers, "On the Architecture of Spacetime Geometry," *Class. Quant. Grav.* **31** (2014) 214002, arXiv:1212.5183 [hep-th].

[10] V. Balasubramanian, B. D. Chowdhury, B. Czech, J. de Boer, and M. P. Heller, "Bulk curves from boundary data in holography," *Phys. Rev.* **D89** no. 8, (2014) 086004, arXiv:1310.4204 [hep-th].

[11] T. Faulkner, M. Guica, T. Hartman, R. C. Myers, and M. Van Raamsdonk, "Gravitation from Entanglement in Holographic CFTs," *JHEP* **1403** (2014) 051, arXiv:1312.7856 [hep-th].

[12] J. Maldacena and L. Susskind, "Cool horizons for entangled black holes," *Fortsch.Phys.* **61** (2013) 781–811, arXiv:1306.0533 [hep-th].

[13] J. D. Bekenstein, "Black holes and entropy," *Physical Review D* **7** no. 8, (1973) 2333.

[14] S. W. Hawking, "Particle Creation by Black Holes," *Commun. Math. Phys.* **43** (1975) 199–220.

[15] G. 't Hooft, "Dimensional reduction in quantum gravity," in *Salamfest 1993:0284-296*, pp. 0284–296. 1993. arXiv:gr-qc/9310026 [gr-qc].

[16] L. Susskind, "The World as a hologram," *J. Math. Phys.* **36** (1995) 6377–6396, arXiv:hep-th/9409089 [hep-th].

[17] R. Bousso, "The Holographic principle," *Rev. Mod. Phys.* **74** (2002) 825–874, arXiv:hep-th/0203101 [hep-th].

[18] G. 't Hooft, "A Planar Diagram Theory for Strong Interactions," *Nucl. Phys.* **B72** (1974) 461.

[19] S. S. Gubser, I. R. Klebanov, and A. M. Polyakov, "Gauge theory correlators from noncritical string theory," *Phys. Lett.* **B428** (1998) 105–114, arXiv:hep-th/9802109 [hep-th].

[20] E. Witten, "Anti-de Sitter space and holography," *Adv. Theor. Math. Phys.* **2** (1998) 253–291, arXiv:hep-th/9802150 [hep-th].

[21] T. Banks, M. R. Douglas, G. T. Horowitz, and E. J. Martinec, "AdS dynamics from conformal field theory," arXiv:hep-th/9808016 [hep-th].

[22] S. B. Giddings, "The Boundary S matrix and the AdS to CFT dictionary," *Phys. Rev. Lett.* **83** (1999) 2707–2710, arXiv:hep-th/9903048 [hep-th].

[23] D. Harlow and D. Stanford, "Operator Dictionaries and Wave Functions in AdS/CFT and dS/CFT," arXiv:1104.2621 [hep-th].

[24] A. Hamilton, D. N. Kabat, G. Lifschytz, and D. A. Lowe, "Holographic representation of local bulk operators," *Phys. Rev.* **D74** (2006) 066009, arXiv:hep-th/0606141 [hep-th].

[25] I. Heemskerk, D. Marolf, J. Polchinski, and J. Sully, "Bulk and Transhorizon Measurements in AdS/CFT," *JHEP* **10** (2012) 165, arXiv:1201.3664 [hep-th].

[26] R. Bousso, B. Freivogel, S. Leichenauer, V. Rosenhaus, and C. Zukowski, "Null Geodesics, Local CFT Operators and AdS/CFT for Subregions," *Phys. Rev.* **D88** (2013) 064057, arXiv:1209.4641 [hep-th].

[27] N. Lashkari, M. B. McDermott, and M. Van Raamsdonk, "Gravitational dynamics from entanglement 'thermodynamics'," *JHEP* **1404** (2014) 195, arXiv:1308.3716 [hep-th].

[28] B. Swingle and M. Van Raamsdonk, "Universality of Gravity from Entanglement," arXiv:1405.2933 [hep-th].

[29] S. W. Hawking and D. N. Page, "Thermodynamics of black holes in anti-de sitter space," *Communications in Mathematical Physics* **87** no. 4, (1983) 577–588.

[30] E. Witten, "Anti-de Sitter space, thermal phase transition, and confinement in gauge theories," *Adv. Theor. Math. Phys.* **2** (1998) 505–532, arXiv:hep-th/9803131 [hep-th].

[31] M. Banados, C. Teitelboim, and J. Zanelli, "Black hole in three-dimensional spacetime," *Physical Review Letters* **69** no. 13, (1992) 1849.

[32] M. Banados, M. Henneaux, C. Teitelboim, and J. Zanelli, "Geometry of the 2+ 1 black hole," *Physical Review D* **48** no. 4, (1993) 1506.

[33] P. Bizon and A. Rostworowski, "On weakly turbulent instability of anti-de Sitter space," *Phys. Rev. Lett.* **107** (2011) 031102, arXiv:1104.3702 [gr-qc].

[34] O. J. C. Dias, G. T. Horowitz, and J. E. Santos, "Gravitational Turbulent Instability of Anti-de Sitter Space," *Class. Quant. Grav.* **29** (2012) 194002, arXiv:1109.1825 [hep-th].

[35] A. Polkovnikov, K. Sengupta, A. Silva, and M. Vengalattore, "Colloquium: Nonequilibrium dynamics of closed interacting quantum systems," *Reviews of Modern Physics* **83** no. 3, (2011) 863.

[36] A. J. Daley, M. Rigol, and D. S. Weiss, "Focus on out-of-equilibrium dynamics in strongly interacting one-dimensional systems," *New J. Phys.* **16** (2014) 095006. http://dx.doi.org/10.1088/1367-2630/16/9/095006.

[37] J. Eisert, M. Friesdorf, and C. Gogolin, "Quantum many-body systems out of equilibrium," *Nat Phys* **11** no. 2, (02, 2015) 124–130. http://dx.doi.org/10.1038/nphys3215.

[38] "Prethermalization and universal dynamics in near-integrable quantum systems," arXiv:1603.09385 [cond-mat.quant-gas].

[39] S. Weigert, "The problem of quantum integrability," *Physica D: Nonlinear Phenomena* **56** no. 1, (1992) 107–119.

[40] J.-S. Caux and J. Mossel, "Remarks on the notion of quantum integrability," *Journal of Statistical Mechanics: Theory and Experiment* **2011** no. 02, (2011) P02023.

[41] H. Bethe, "Zur theorie der metalle. eigenwerte und eigenfunktionen atomkete," *Z. Phys* **71** (1931) 205.

[42] M. Rigol, V. Dunjko, V. Yurovsky, and M. Olshanii, "Relaxation in a completely integrable many-body quantum system: An *Ab Initio* study of the dynamics of the highly excited states of 1d lattice hard-core bosons," *Physical Review Letters* **98** no. 5, (2007) .

[43] T. Kinoshita, T. Wenger, and D. S. Weiss, "A quantum newton's cradle," *Nature* **440** no. 7086, (2006) 900–903.

[44] J. de Boer and D. Engelhardt, "Comments on Thermalization in 2D CFT," arXiv:1604.05327 [hep-th].

[45] D. Engelhardt, "Quench dynamics in confined 1 + 1-dimensional systems," *J. Phys.* **A49** no. 12, (2016) 12LT01, arXiv:1502.02678 [hep-th].

[46] D. Engelhardt, B. Freivogel, and N. Iqbal, "Electric fields and quantum wormholes," *Phys. Rev.* **D92** no. 6, (2015) 064050, arXiv:1504.06336 [hep-th].

[47] M. Srednicki, "Chaos and quantum thermalization," *Physical Review E* **50** no. 2, (1994) 888–901.

[48] J. M. Deutsch, "Quantum statistical mechanics in a closed system," *Physical Review A* **43** no. 4, (1991) 2046–2049.

[49] M. Rigol, V. Dunjko, and M. Olshanii, "Thermalization and its mechanism for generic isolated quantum systems," *Nature* **452** no. 7189, (04, 2008) 854–858.

[50] M. Rigol, "Alternatives to eigenstate thermalization," *Physical Review Letters* **108** no. 11, (2012) .

[51] P. Calabrese and J. L. Cardy, "Time-dependence of correlation functions following a quantum quench," *Phys. Rev. Lett.* **96** (2006) 136801, arXiv:cond-mat/0601225 [cond-mat].

[52] P. Calabrese and J. Cardy, "Quantum Quenches in Extended Systems," *J. Stat. Mech.* **0706** (2007) P06008, arXiv:0704.1880 [cond-mat.stat-mech].

[53] P. Calabrese and J. Cardy, "Entanglement and correlation functions following a local quench: a conformal field theory approach," *J. Stat. Mech.* (2007) P10004, arXiv:0708.3750 [cond-mat.stat-mech].

[54] T. Hartman and J. Maldacena, "Time Evolution of Entanglement Entropy from Black Hole Interiors," *JHEP* **1305** (2013) 014, arXiv:1303.1080 [hep-th].

[55] J. Cardy, "Thermalization and Revivals after a Quantum Quench in Conformal Field Theory," *Phys. Rev. Lett.* **112** (2014) 220401, arXiv:1403.3040 [cond-mat.stat-mech].

[56] K. Kuns and D. Marolf, "Non-Thermal Behavior in Conformal Boundary States," *JHEP* **09** (2014) 082, arXiv:1406.4926 [cond-mat.stat-mech].

[57] C. T. Asplund, A. Bernamonti, F. Galli, and T. Hartman, "Entanglement Scrambling in 2d Conformal Field Theory," *JHEP* **09** (2015) 110, arXiv:1506.03772 [hep-th].

[58] P. Calabrese and J. Cardy, "Quantum quenches in 1+1 dimensional conformal field theories," arXiv:1603.02889 [cond-mat.stat-mech].

[59] V. V. Bazhanov, S. L. Lukyanov, and A. B. Zamolodchikov, "Integrable structure of conformal field theory, quantum KdV theory and thermodynamic Bethe ansatz," *Commun. Math. Phys.* **177** (1996) 381–398, arXiv:hep-th/9412229 [hep-th].

[60] J. Cardy, "Quantum Quenches to a Critical Point in One Dimension: some further results," *J. Stat. Mech.* **1602** no. 2, (2016) 023103, arXiv:1507.07266 [cond-mat.stat-mech].

[61] G. Mandal, R. Sinha, and N. Sorokhaibam, "Thermalization with chemical potentials, and higher spin black holes," *JHEP* **08** (2015) 013, arXiv:1501.04580 [hep-th].

[62] G. Mandal, S. Paranjape, and N. Sorokhaibam, "Thermalization in 2D critical quench and UV/IR mixing," arXiv:1512.02187 [hep-th].

[63] P. Calabrese and J. L. Cardy, "Evolution of entanglement entropy in one-dimensional systems," *J. Stat. Mech.* **0504** (2005) P04010, arXiv:cond-mat/0503393 [cond-mat].

[64] P. Calabrese and J. Cardy, "Entanglement entropy and conformal field theory," *J. Phys.* **A42** (2009) 504005, arXiv:0905.4013 [cond-mat.stat-mech].

[65] V. Balasubramanian, A. Bernamonti, J. de Boer, N. Copland, B. Craps, E. Keski-Vakkuri, B. Muller, A. Schafer, M. Shigemori, and W. Staessens, "Thermalization of Strongly Coupled Field Theories," *Phys. Rev. Lett.* **106** (2011) 191601, arXiv:1012.4753 [hep-th].

[66] V. Balasubramanian, A. Bernamonti, J. de Boer, N. Copland, B. Craps, E. Keski-Vakkuri, B. Muller, A. Schafer, M. Shigemori, and W. Staessens, "Holographic Thermalization," *Phys. Rev.* **D84** (2011) 026010, arXiv:1103.2683 [hep-th].

[67] P. Caputa, G. Mandal, and R. Sinha, "Dynamical entanglement entropy with angular momentum and U(1) charge," *JHEP* **11** (2013) 052, arXiv:1306.4974 [hep-th].

[68] H. Liu and S. J. Suh, "Entanglement growth during thermalization in holographic systems," *Phys. Rev.* **D89** no. 6, (2014) 066012, arXiv:1311.1200 [hep-th].

[69] M. Banados, "Three-dimensional quantum geometry and black holes," arXiv:hep-th/9901148 [hep-th]. [AIP Conf. Proc.484,147(1999)].

[70] J. Balog, L. Feher, and L. Palla, "Coadjoint orbits of the Virasoro algebra and the global Liouville equation," *Int. J. Mod. Phys.* **A13** (1998) 315–362, arXiv:hep-th/9703045 [hep-th].

[71] E. J. Martinec, "Conformal field theory, geometry, and entropy," arXiv:hep-th/9809021 [hep-th].

[72] W. Donnelly, D. Marolf, and E. Mintun, "Combing gravitational hair in 2 + 1 dimensions," *Class. Quant. Grav.* **33** no. 2, (2016) 025010, arXiv:1510.00672 [hep-th].

[73] "Symplectic and Killing symmetries of AdS_3 gravity: holographic vs boundary gravitons," *JHEP* **01** (2016) 080, arXiv:1511.06079 [hep-th].

[74] M. M. Sheikh-Jabbari and H. Yavartanoo, "On 3d Bulk Geometry of Virasoro Coadjoint Orbits: Orbit invariant charges and Virasoro hair on locally AdS3 geometries," arXiv:1603.05272 [hep-th].

[75] T. Takayanagi, "Holographic Dual of BCFT," *Phys. Rev. Lett.* **107** (2011) 101602, arXiv:1105.5165 [hep-th].

[76] M. Fujita, T. Takayanagi, and E. Tonni, "Aspects of AdS/BCFT," *JHEP* **11** (2011) 043, arXiv:1108.5152 [hep-th].

[77] P. D. Francesco, P. Mathieu, and D. Sénéchal, *Conformal Field Theory, Graduate Texts in Contemporary Physics*. Springer, New York, 1999.

[78] T. A. Driscoll and L. N. Trefethen, *Schwarz-Christoffel Mapping*, vol. 8. Cambridge University Press, 2002.

[79] J. de Boer and J. I. Jottar *To appear* .

[80] J. de Boer and J. I. Jottar, "Boundary Conditions and Partition Functions in Higher Spin AdS_3/CFT_2," arXiv:1407.3844 [hep-th].

[81] E. Witten, "Multitrace operators, boundary conditions, and AdS / CFT correspondence," arXiv:hep-th/0112258 [hep-th].

[82] A. Sever and A. Shomer, "A Note on multitrace deformations and AdS/CFT," *JHEP* **07** (2002) 027, arXiv:hep-th/0203168 [hep-th].

[83] E. Date, M. Jimbo, M. Kashiwara, and T. Miwa, "Transformation groups for soliton equations —euclidean lie algebras and reduction of the kp hierarchy," *Publ. Res. Inst. Math. Sci.* **18** (1982) 1077–1110. http://doi.org/10.2977/prims/1195183297.

[84] M. Jimbo and T. Miwa, "Solitons and infinite dimensional lie algebras," *Publ. RIMS, Kyoto Univ* **19** (1983) 943–1001.

[85] V. G. Drinfeld and V. V. Sokolov, "Lie algebras and equations of korteweg-de vries type," *Journal of Soviet mathematics* **30** no. 2, (1985) 1975–2036.

[86] A. L. Fitzpatrick, J. Kaplan, and M. T. Walters, "Virasoro Conformal Blocks and Thermality from Classical Background Fields," *JHEP* **11** (2015) 200, arXiv:1501.05315 [hep-th].

[87] O. J. C. Dias, G. T. Horowitz, D. Marolf, and J. E. Santos, "On the Nonlinear Stability of Asymptotically Anti-de Sitter Solutions," *Class. Quant. Grav.* **29** (2012) 235019, arXiv:1208.5772 [gr-qc].

[88] M. Maliborski and A. Rostworowski, "Time-Periodic Solutions in an Einstein AdS–Massless-Scalar-Field System," *Phys. Rev. Lett.* **111** (2013) 051102, arXiv:1303.3186 [gr-qc].

[89] K. Skenderis and B. C. van Rees, "Real-time gauge/gravity duality," *Phys. Rev. Lett.* **101** (2008) 081601, arXiv:0805.0150 [hep-th].

[90] K. Skenderis and B. C. van Rees, "Real-time gauge/gravity duality: Prescription, Renormalization and Examples," *JHEP* **05** (2009) 085, arXiv:0812.2909 [hep-th].

[91] A. Zamolodchikov, "Integrable field theory from conformal field theory," *Adv. Stud. Pure Math* **19** (1989) 641.

[92] V. V. Bazhanov, S. L. Lukyanov, and A. B. Zamolodchikov, "Integrable structure of conformal field theory. 2. Q operator and DDV equation," *Commun. Math. Phys.* **190** (1997) 247–278, arXiv:hep-th/9604044 [hep-th].

[93] V. V. Bazhanov, S. L. Lukyanov, and A. B. Zamolodchikov, "Integrable structure of conformal field theory iii. the yang–baxter relation," *Communications in mathematical physics* **200** no. 2, (1999) 297–324.

[94] A. B. Zamolodchikov, "Two-point correlation function in scaling lee-yang model," *Nuclear Physics B* **348** no. 3, (1991) 619–641.

[95] E. H. Lieb and W. Liniger, "Exact analysis of an interacting bose gas. i. the general solution and the ground state," *Physical Review* **130** no. 4, (1963) 1605.

[96] M. Kormos, G. Mussardo, and A. Trombettoni, "Expectation values in the lieb-liniger bose gas," *Physical review letters* **103** no. 21, (2009) 210404.

[97] M. Kormos, G. Mussardo, and A. Trombettoni, "One-dimensional lieb-liniger bose gas as nonrelativistic limit of the sinh-gordon model," *Physical Review A* **81** no. 4, (2010) 043606.

[98] M. Girardeau, "Relationship between systems of impenetrable bosons and fermions in one dimension," *Journal of Mathematical Physics* **1** no. 6, (1960) 516–523.

[99] N. Ishibashi, "The boundary and crosscap states in conformal field theories," *Modern Physics Letters A* **4** no. 03, (1989) 251–264.

[100] T. Onogi and N. Ishibashi, "Conformal field theories on surfaces with boundaries and crosscaps," *Modern Physics Letters A* **4** no. 02, (1989) 161–168.

[101] J. L. Cardy, "Boundary conditions, fusion rules and the verlinde formula," *Nuclear Physics B* **324** no. 3, (1989) 581–596.

[102] B. Hsu and E. Fradkin, "Universal Behavior of Entanglement in 2D Quantum Critical Dimer Models," *J. Stat. Mech.* **1009** (2010) P09004, arXiv:1006.1361 [cond-mat.stat-mech].

[103] M. Oshikawa, "Boundary Conformal Field Theory and Entanglement Entropy in Two-Dimensional Quantum Lifshitz Critical Point," arXiv:1007.3739 [cond-mat.stat-mech].

[104] L. C. Venuti, H. Saleur, and P. Zanardi, "Universal subleading terms in ground-state fidelity from boundary conformal field theory," *Physical Review B* **79** no. 9, (2009) 092405.

[105] I. Affleck and A. W. Ludwig, "Universal noninteger "ground-state degeneracy"in critical quantum systems," *Physical Review Letters* **67** no. 2, (1991) 161.

[106] J. L. Cardy, "Conformal Invariance and Surface Critical Behavior," *Nucl. Phys.* **B240** (1984) 514–532.

[107] J. Cardy, *Finite-size scaling*, vol. 2. Elsevier, 2012.

[108] M. Cazalilla, "Bosonizing one-dimensional cold atomic gases," *Journal of Physics B: Atomic, Molecular and Optical Physics* **37** no. 7, (2004) S1.

[109] S. Ghoshal and A. B. Zamolodchikov, "Boundary S matrix and boundary state in two-dimensional integrable quantum field theory," *Int. J. Mod. Phys.* **A9** (1994) 3841–3886, arXiv:hep-th/9306002 [hep-th]. [Erratum: Int. J. Mod. Phys.A9,4353(1994)].

[110] J. M. Maldacena, "Eternal black holes in anti-de Sitter," *JHEP* **0304** (2003) 021, arXiv:hep-th/0106112 [hep-th].

[111] B. Swingle, "Entanglement renormalization and holography," *Phys. Rev. D* **86** (Sep, 2012) 065007, arXiv:0905.1317 [cond-mat].

[112] A. Einstein, B. Podolsky, and N. Rosen, "Can quantum mechanical description of physical reality be considered complete?," *Phys.Rev.* **47** (1935) 777–780.

[113] A. Einstein and N. Rosen, "The Particle Problem in the General Theory of Relativity," *Phys.Rev.* **48** (1935) 73–77.

[114] L. Susskind, "New Concepts for Old Black Holes," arXiv:1311.3335 [hep-th].

[115] "Holographic EPR Pairs, Wormholes and Radiation," *JHEP* **1310** (2013) 211, arXiv:1308.3695 [hep-th].

[116] L. Susskind, "Butterflies on the Stretched Horizon," arXiv:1311.7379 [hep-th].

[117] L. Susskind, "Computational Complexity and Black Hole Horizons," arXiv:1402.5674 [hep-th].

[118] L. Susskind, "Addendum to Computational Complexity and Black Hole Horizons," arXiv:1403.5695 [hep-th].

[119] D. Stanford and L. Susskind, "Complexity and Shock Wave Geometries," *Phys.Rev.* **D90** no. 12, (2014) 126007, arXiv:1406.2678 [hep-th].

[120] L. Susskind and Y. Zhao, "Switchbacks and the Bridge to Nowhere," arXiv:1408.2823 [hep-th].

[121] L. Susskind, "ER=EPR, GHZ, and the Consistency of Quantum Measurements," arXiv:1412.8483 [hep-th].

[122] D. A. Roberts, D. Stanford, and L. Susskind, "Localized shocks," *JHEP* **1503** (2015) 051, arXiv:1409.8180 [hep-th].

[123] L. Susskind, "Entanglement is not Enough," arXiv:1411.0690 [hep-th].

[124] K. Jensen and A. Karch, "Holographic Dual of an Einstein-Podolsky-Rosen Pair has a Wormhole," *Phys.Rev.Lett.* **111** no. 21, (2013) 211602, arXiv:1307.1132 [hep-th].

[125] J. Sonner, "Holographic Schwinger Effect and the Geometry of Entanglement," *Phys.Rev.Lett.* **111** no. 21, (2013) 211603, arXiv:1307.6850 [hep-th].

[126] K. Jensen and J. Sonner, "Wormholes and entanglement in holography," *Int.J.Mod.Phys.* **D23** no. 12, (2014) 1442003, arXiv:1405.4817 [hep-th].

[127] K. Jensen, A. Karch, and B. Robinson, "Holographic dual of a Hawking pair has a wormhole," *Phys.Rev.* **D90** no. 6, (2014) 064019, arXiv:1405.2065 [hep-th].

[128] H. Gharibyan and R. F. Penna, "Are entangled particles connected by wormholes? Evidence for the ER=EPR conjecture from entropy inequalities," *Phys.Rev.* **D89** no. 6, (2014) 066001, arXiv:1308.0289 [hep-th].

[129] K. Papadodimas and S. Raju, "Comments on the Necessity and Implications of State-Dependence in the Black Hole Interior," arXiv:1503.08825 [hep-th].

[130] D. Garfinkle and A. Strominger, "Semiclassical Wheeler wormhole production," *Phys.Lett.* **B256** (1991) 146–149.

[131] C. W. Misner and J. A. Wheeler, "Classical physics as geometry: Gravitation, electromagnetism, unquantized charge, and mass as properties of curved empty space," *Annals Phys.* **2** (1957) 525–603.

[132] N. Arkani-Hamed, L. Motl, A. Nicolis, and C. Vafa, "The String landscape, black holes and gravity as the weakest force," *JHEP* **0706** (2007) 060, arXiv:hep-th/0601001 [hep-th].

[133] T. Banks and N. Seiberg, "Symmetries and Strings in Field Theory and Gravity," *Phys.Rev.* **D83** (2011) 084019, arXiv:1011.5120 [hep-th].

[134] W. Israel, "Thermo field dynamics of black holes," *Phys.Lett.* **A57** (1976) 107–110.

[135] T. Andrade, S. Fischetti, D. Marolf, S. F. Ross, and M. Rozali *JHEP* **1404** (2014) 023, arXiv:1312.2839 [hep-th].

[136] S. Leichenauer, "Disrupting Entanglement of Black Holes," *Phys.Rev.* **D90** no. 4, (2014) 046009, arXiv:1405.7365 [hep-th].

[137] D. Harlow, "Aspects of the Papadodimas-Raju Proposal for the Black Hole Interior," *JHEP* **1411** (2014) 055, arXiv:1405.1995 [hep-th].

[138] N. Arkani-Hamed, A. G. Cohen, and H. Georgi, "(De)constructing dimensions," *Phys.Rev.Lett.* **86** (2001) 4757–4761, arXiv:hep-th/0104005 [hep-th].

[139] D. Marolf and J. Polchinski, "Gauge/Gravity Duality and the Black Hole Interior," *Phys.Rev.Lett.* **111** (2013) 171301, arXiv:1307.4706 [hep-th].

[140] V. Balasubramanian, M. Berkooz, S. F. Ross, and J. Simon, "Black Holes, Entanglement and Random Matrices," *Class.Quant.Grav.* **31** (2014) 185009, arXiv:1404.6198 [hep-th].

[141] S. S. Gubser, "Breaking an Abelian gauge symmetry near a black hole horizon," *Phys.Rev.* **D78** (2008) 065034, arXiv:0801.2977 [hep-th].

[142] S. A. Hartnoll, C. P. Herzog, and G. T. Horowitz, "Building a Holographic Superconductor," *Phys.Rev.Lett.* **101** (2008) 031601, arXiv:0803.3295 [hep-th].

[143] S. A. Hartnoll, C. P. Herzog, and G. T. Horowitz, "Holographic Superconductors," *JHEP* **0812** (2008) 015, arXiv:0810.1563 [hep-th].

[144] K. Papadodimas and S. Raju, "Local Operators in the Eternal Black Hole," arXiv:1502.06692 [hep-th].

[145] S. H. Shenker and D. Stanford, "Black holes and the butterfly effect," *JHEP* **1403** (2014) 067, arXiv:1306.0622 [hep-th].

[146] J. Polchinski, "Monopoles, duality, and string theory," *Int.J.Mod.Phys.* **A19S1** (2004) 145–156, arXiv:hep-th/0304042 [hep-th].

[147] M. Campostrini and E. Vicari, "Quantum critical behavior and trap-size scaling of trapped bosons in a one-dimensional optical lattice," *Physical Review A* **81** no. 6, (2010) 063614.

[148] M. Campostrini and E. Vicari, "Critical behavior and scaling in trapped systems," *Physical review letters* **102** no. 24, (2009) 240601.

[149] M. Campostrini and E. Vicari, "Equilibrium and off-equilibrium trap-size scaling in one-dimensional ultracold bosonic gases," *Physical Review A* **82** no. 6, (2010) 063636.

[150] M. Campostrini, A. Pelissetto, and E. Vicari, "Finite-size scaling at quantum transitions," *Physical Review B* **89** no. 9, (2014) 094516.

[151] M. P. Fisher, P. B. Weichman, G. Grinstein, and D. S. Fisher, "Boson localization and the superfluid-insulator transition," *Physical Review B* **40** no. 1, (1989) 546.